

1 Deep Underground Neutrino Experiment (DUNE)
2 Technical Proposal

3 **13 April 2018: Final draft of the TP volumes due**
4 Volume 1: *Executive Summary*

5 April 6, 2018

1 **Contents**

2	Contents	i
3	List of Figures	ii
4	List of Tables	iii
5	1 Calibration Strategy	1
6	1.1 Introduction	1
7	1.2 Physics Requirements for Calibration	4
8	1.2.1 Long-baseline physics	4
9	1.2.2 Supernova physics	5
10	1.2.3 Exotic Physics	7
11	1.3 External Measurements Relevant to Calibration	8
12	1.3.1 Measurements of detector response model	8
13	1.3.2 Measurements of relevant high-level physics quantities	11
14	1.3.3 Future Measurements	12
15	1.4 Existing Calibration Sources	13
16	1.4.1 Cosmic Rays	13
17	1.4.2 Neutrino-induced interactions	18
18	1.4.3 Argon 39	20
19	1.4.4 Instrumentation and Monitoring Data	22
20	1.5 Dual Phase Considerations for Calibration	26
21	1.6 Calibration Systems Under Consideration for DUNE	28
22	1.6.1 Calibration Penetrations	28
23	1.6.2 Laser Systems	30
24	1.6.3 Radioactive Source Deployment System	33
25	1.6.4 External Neutron Source	35
26	1.6.5 Photon Detection Monitoring System	38
27	1.6.6 Cosmic Ray Tagger	40
28	1.7 Calibration Summary	42
29	1.7.1 Path to the TDR	42
30	References	45

2 List of Figures

3	1.1	Categories of measurements provided by Calibration.	2
4	1.2	6
5	1.3	Sample distortion that may be difficult to detect with cosmic rays	17
6	1.4	Impact of detector effects on ^{39}Ar beta decay electron energy spectrum	21
7	1.5	Simulated effects of space charge on distortions in reconstructed ionization electron	
8		cluster positions in a DP detector module	26
9	1.6	Top view of the SP detector module cryostat showing various penetrations. Highlighted	
10		in black circles are multi-purpose calibration penetrations. The orange dots are TPC	
11		signal cable penetrations. The blue ports are detector support system (DSS) penetra-	
12		tions. The orange ports are TPC signal cable penetrations. The larger purple ports at	
13		the four corners of the cryostat are manholes.	28
14	1.7	Elastic scattering cross sections on argon isotopes	36
15	1.8	h	36
16	1.9	UV-light photon calibration system in the DUNE 35 ton prototype	39

² List of Tables

³	1.1	Atmospheric and beam neutrino and antineutrino event rates per year	18
⁴	1.2	Key Calibration milestones leading to TDR	43

¹

2 **Todo list**

3	references for 35t is "M. Thiesse, Ph.D. Thesis, University of Sheffield, 2018)" and LArIAT? . . .	15
4	increases in the field cause increases in drift speed? pls clarify	24
5	Need to confirm this number	24
6	previous sentence needs work; I cannot parse it	24
7	electric field, E field or E-field? We have to decide for entire TP!	30
8	I don't find citation bib:Triumpf:Nickelsource (anne)	33
9	need to add reference: Double Chooz: NEAR DETECTOR TECHNICAL DESIGN REPORT	
10	EDMS ID:I-028812 ; DocDB ID: 3403-V5 Pages 198 - 223 (Anne can't find proper ref for	
11	this)	33
12	(NOTE: PUT IN EFFECTIVE CROSS SECTION)	35
13	NOTE: PUT IN PLOTS FOR ELASTIC	35
14	Resolution of plots too bad and labels/titles not readable; get updated plots	35
15	I don't find cit for ref:ENDF -anne	35
16	add more studies	37
17	Uploaded beginning of file to here 4/2/18 Anne; still to add in more sections	38
18	This is for SP only; Need to clarify that through out the section. The PDS for DP system is	
1	covered under the DP-PDS consortium chapter. Will need to state that and link it from here.	38

Chapter 1

Calibration Strategy

1.1 Introduction

The DUNE far detector (FD) presents a unique challenge for calibration in many ways. Not only because of its size—the largest LArTPC ever constructed – but also because of its depth. It differs both from existing long-baseline neutrino detectors, and existing LArTPCs. Also, the deep underground location results in low cosmic ray rates limiting the usage of it as a calibration source. Another important difference is that DUNE does not as yet have a near detector design and, unlike MINOS and NOvA, the near detector is unlikely to be very much like the FD.

Like any LArTPC, DUNE has as a great advantage precision tracking and ultra-clean target medium, but, to fully exploit this will require significant challenges in understanding its detector response. This challenge is driven by the inherently highly convolved detector response model and strong correlations that exist between various calibration quantities. For example, the drift vertex of a track, the drift distance, the initial time the track occurs (t_0) and the drift velocity are all highly correlated. In turn, the drift velocity depends on the electric field. The electric field itself may have local variations in space or in time for an enormous detector operating for multiple decades. The determination of energy associated to an event of interest will depend on the simulation model, associated parameters, non-trivial correlations between the parameters and spatial and temporal dependence of those parameters. These variations in parameters occur since the detector is not static. Changes can be abrupt (e.g. noise, a broken resistor in the field cage), or ongoing (e.g. exchange of fluid through volume, ion accumulation). Unfortunately, the relevant calibration sampling timescales of such changes are not currently known, though ongoing and past experiments may be able to place reasonable limits on how often events may occur.

A convincing measurement of CP violation, or a resolution of the neutrino mass ordering, will require a demonstration that the overall detector response is well understood, and can be extrapolated across the entire physics regions of interest. This document will describe a strategy for detector calibration for both SP modules and DP modules using dedicated FD systems and/or existing calibration sources. A large portion of the calibration work reported here is done under

the joint single-phase (SP) and dual-phase (DP) Calibration task force (TF) group formed in Fall 2017. Calibration sources and systems provide measurements of the detector response model parameters, or provide tests of the response model. Figure 1.1 shows the broad range of categories of measurements calibrations can provide. In addition to this, calibration measurements also provide corrections applied to data, data-driven efficiencies, systematics and particle responses. Figure 1.1 also lists some of the critical calibration parameters for DUNE's detector response model for either SP or DP. Due to the significant interdependencies of many parameters (recombination, drift velocity, electric field), a calibration strategy will either need to iteratively measure parameters, and/or find sources which break these correlations.

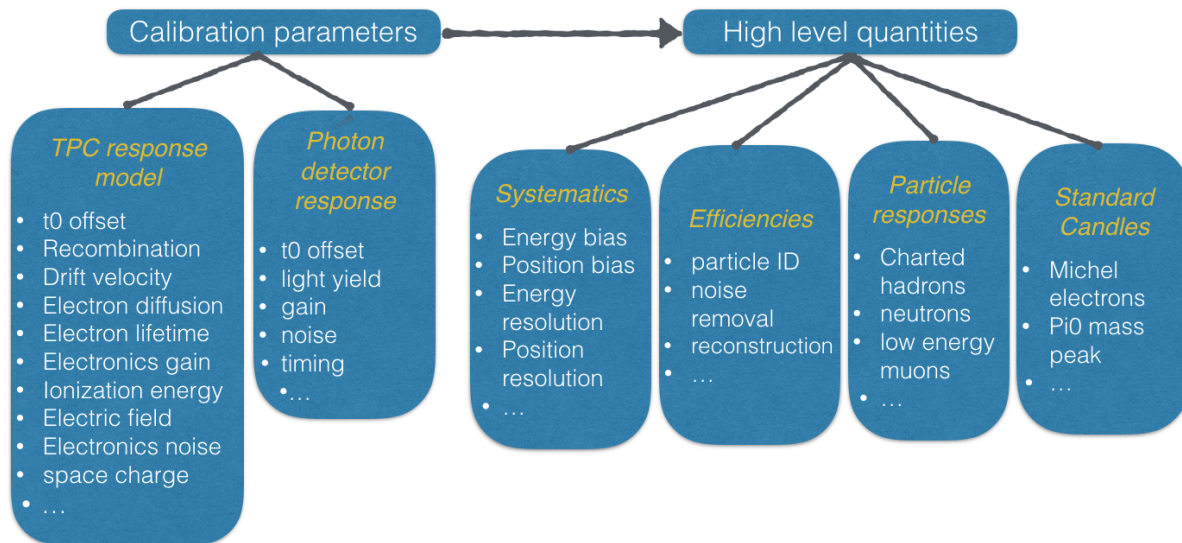


Figure 1.1: Categories of measurements provided by Calibration.

The systematic uncertainties on high level physics quantities drive how precisely each parameter need to be measured. For example, how precisely will the drift velocity need to be measured to know fiducial volume better than 1%? What does 1% energy bias mean for electron drift-lifetime and electronics calibration measurements? Section 1.2 describes the physics requirements for calibration for long-baseline, supernovae and other physics such as nucleon decay and exotic searches. In general, the calibration program must provide measurements at the few percent or better level, and must also provide sufficient redundancy in the measurement program.

Section 1.3 describes calibration measurements from other LAr experiments that are of relevant for DUNE. This includes both past measurements (e.g., ArgoNeuT, DUNE 35 ton prototype, MicroBooNE, LArIAT), anticipated measurements from ongoing and future experiments (e.g., MicroBooNE, ProtoDUNE) as well as from small scale LArTPC test stands. Some parameters, like the argon ionization energy, are believed to be universal and have been measured ex-situ. ProtoDUNE and previous measurements provide independent, critical tests of the response model, where the choice of parameterization and values correctly reproduces real detector data. However informative, not all of the previous ex-situ measurements will be directly extrapolatable to DUNE.

Section 1.4 describes existing calibration sources, their limitations and remaining studies necessary for the TDR. Existing calibration sources include (beam or atmospheric) neutrino-induced samples,

cosmic rays, argon isotopes and instrumentation devices such as liquid argon purity monitors, temperature and current monitors. For example, drift velocity depends on temperature (and electric field), so measurements of temperature reduce the interdependencies in understanding drift velocity. While there are many existing calibration sources, each source comes with its own challenges. We further distinguish between sources which are used to measure a response model parameter, and measurements which test the response model. For example, electrons from muon decay (Michel electrons) are very useful to study the detector response to low energy electrons (~ 50 MeV). However, low-energy electrons have major reconstruction challenges due to the loss of charge from radiative photons as demonstrated in MicroBooNE [2]. In terms of source category, Michel electrons are considered as an important, independent, and necessary test of the TPC energy response model, and not as a measurement of a particular response parameter.

[sec:DP](#)
Section 1.5 describes some specific calibration-related considerations for DP. One of the biggest challenges for DP is the 12 m long single drift path and ion accumulation at the liquid-gas interface.

[sec:extsystems](#)
Section 1.6 describes dedicated external calibration systems currently under consideration for DUNE to perform calibrations that cannot be achieved fully from existing sources or external measurements. For each system considered, a reference design is described along with motivation, possible measurements and remaining studies for the TDR. All the systems proposed are currently being actively discussed in the Calibration Task Force and were agreed as critical systems by the DUNE collaboration. While the proposed external calibration systems are being finalized, the calibration TF focused on finalizing the feedthrough penetration design for the SP module and made necessary accommodations for calibration systems. [sec:Fls](#)
The current cryostat penetration design for SP module calibrations is described in Section 1.6.1. The TF will soon start focusing on DP module design and accommodations in terms of calibration penetrations. Under current assumptions, the calibration strategy and proposed calibration systems described in this document are applicable to both SPs and DPs.

[sec:calibsum](#)
Section 1.7 provides a summary of the document along with future steps for calibration and a path to TDR.

1.2 Physics Requirements for Calibration

DUNE has a broad physics program which includes long baseline physics, supernova physics, nucleon decay and other exotic searches. The physics processes which lead to the formation of these signals and the detector effects which impact their propagation must be carefully understood in order to perform adequate calibrations as it ultimately impacts the detector's energy response. In addition to measurements of specific detector effects, studies that address energy resolution performed with various sources offer a higher level evaluation of detector performance which can be used to assess the impact on physics analyses and/or verify specific aspects of the detector response model relevant for that physics.

In addition to calibration, several other categories of effects can impact long baseline physics such as the neutrino interaction model, insufficient calibration, or reconstruction pathologies. For this note, we take as a target that calibration, by itself, needs to be sufficient for DUNE's program; other issues which limit the physics program are out of scope and can only amplify the overall error budget. Section 1.2.1 describes the calibration-driven physics requirements for the long baseline program, Section 1.2.2 describes the supernova physics program which relies on low-energy interactions, and Section 1.2.3 describes exotic physics model searches, including nucleon decay.

1.2.1 Long-baseline physics

DUNE's LBL program uses measurements of ν_e , $\bar{\nu}_e$ appearance and ν_μ disappearance, to probe for new physics with neutrinos, including a search for CP violation (CPV), and the mass hierarchy. Additional far detector physics includes measurements with atmospheric neutrinos, ν_τ appearance, and non-standard matter interactions or other effects. These programs all rely on neutrinos of energies 0.2-10 GeV.

In the physics volume of the DUNE CDR [3], Figure 3.23 shows that increasing the uncertainties on the ν_e event rate from 2% overall¹ to 3% results in a 50% longer run period. The CDR also assumes that the fiducial volume is understood at the 1% level. Thus, calibration information needs to provide approximately 1-2% understanding of normalization, energy and position resolution within the detector. Later studies [4] expanded the simple treatment of energy presented above. In particular, 1% bias on the lepton energy has a significant impact on the sensitivity to CPV. A 3% bias in the hadronic state (excluding neutrons), is important as well, as the Bjorken y distribution for neutrinos and antineutrinos are quite different, and a larger fraction of the antineutrino's energy will go into the hadronic state. Finally, while studies largely consider a single, absolute energy scale, relative spatial differences across the enormous DUNE FD volume will need to be monitored and corrected; this is also true for changes which occur in time.

Some of the primary requirements for LBL physics include neutrino vertex reconstruction, par-

¹This uncertainty is an uncorrelated normalization uncertainty on the far detector ν_e rate in a four sample FD fit that assumes reasonable near detector constraints on flux and cross sections.

particle identification, electromagnetic shower energy measurement, e/γ separation, and momentum measurements (e.g. using particle range or Multiple Coulomb Scattering). A number of in-situ calibration sources will be required to address these broad range of requirements. Michel electrons, neutral pions and radioactive sources (both intrinsic and external) are valuable for calibrating detector response to electromagnetic activity in the tens to hundreds of MeV energy range. Stopping protons and muons from cosmic rays or beam interactions form an important calibration source for calorimetric reconstruction and particle identification. ProtoDUNE, as a dedicated test beam experiment, provides critical measurements to characterize and validate particle identification strategies in a 1 kt scale detector and will be an essential input to the overall program. Dedicated calibration systems, like laser-based ones, can provide in-situ full volume measurements of electric field distortions. The electric field is a critical aspect of calibration, as estimates of calorimetric response and particle identification depend on electric field through recombination.

Spatial deformations within the detector can also impact the energy estimator. Particles in the detector will repeatedly (elastic) Coulomb scatter with the liquid resulting in small, randomized deviations to their path. Multiple Coulomb Scattering (MCS) is used estimate the particles initial energy, but relies on a known distance the particles traveled. If the distance is different than expectation due to misalignments or spatial deformations caused by electric field, then this may bias the estimator. The stringent physics requirements on energy scale and fiducial volume also put similarly stringent requirements on detector physics quantities such as electric field, drift velocity, electron lifetime, and the time dependences of these quantities.

The calibration group in conjunction with the LBL, Simulation and Reconstruction groups will develop the necessary tools to propagate detector physics effects into LBL physics. Some of the studies planned include quantifying (at truth level) the impact of drift field distortions (due to ionization and non-ionization sources such as misalignment) on muon, electron, pion, and proton tracks. The impact should also be assessed for overall calorimetry including below particle tracking or ID threshold. Also, quantifying the relative importance of electromagnetic shower photons below pair production threshold will be pursued.

1.2.2 Supernova physics

The DUNE Supernova burst and low-energy (supernova neutrino burst and low energy (SNB/LE)) neutrino physics focuses on physics that can be done with neutrinos with energies of less than about 100 MeV. The primary physics topic is detection of the burst of neutrinos from a core-collapse supernova, with potentially very rich physics and astrophysics yield. The expected signal is a burst of neutrinos of all flavors in the few- to few-tens-of-MeV range within tens of seconds, of which the component detectable by the DUNE LArTPC is primarily ν_e . Overall, one wants to know the energy, flavor and time structure of the burst. The SNB/LE physics also considers solar neutrinos (energies up to ~ 15 MeV) and the diffuse supernova neutrino flux (DSNB) which should have roughly similar properties to the supernova neutrino burst (SNB) flux, but much lower rate. For the latter two physics topics, the main concern is the background.

These events present specific reconstruction and calibration challenges. Supernova neutrino events, due to their low energies, will manifest themselves as small, perhaps few tens of cm, stub-like

tracks from electrons (or positrons from the rarer $\bar{\nu}_e$ interactions). Events from ν_e charged-current interactions, $\nu_e + {}^{40}\text{Ar} \rightarrow e^- + {}^{40}\text{K}^*$, are likely to be accompanied by de-excitation products – gamma rays and/or ejected nucleons, as shown in Figure 1.2. Gamma-rays are in principle observable via energy deposition from Compton scattering, which will show up as small charge blips in the time projection chamber (TPC). Ejected nucleons may result in loss of observed energy for the event. Elastic scattering on electrons will result in single scattered electrons, and single gamma rays may result from NC excitations of the argon nucleus. Each event category has, in principle, a distinctive signature. In each case, observable energy is shared between different charge clusters and types of energy depositions.

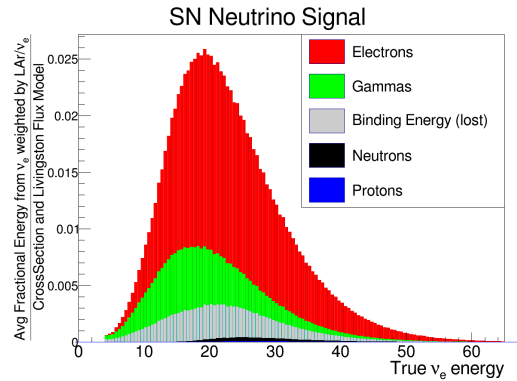


Figure 1.2: Expected SNB electron neutrino energy spectrum and contributions of emitted particle types to the visible energy.

fig:SNB

The canonical reconstruction task is to identify the interaction channel, the neutrino flavor for CC events, and to determine the four-momentum of the incoming neutrino; this overall task is the same for low-energy events as for high-energy ones. The challenge is to reconstruct the properties of the lepton (if present), and to the extent possible, to tag the interaction channel by the pattern of final-state particles.

Calibration of absolute energy scale and understanding of energy resolution will be important for interpretation of the signal. We expect nominally $\sim 20\%$ resolution, although better would be desirable for resolution of supernova spectral features. Furthermore, a sample of data events of known properties with which to validate efficiencies of selection and reconstruction algorithms would be very valuable.

Given that the signal is expected to be uniformly distributed within the detector, absolute position resolution may not be critical (and events are likely to be widely separated in space for all but the very closest supernovae). However, good position resolution of photon detection is needed for good energy resolution, via correction for attenuation of charge during drift. Photon detectors in general may provide useful trigger information (and perhaps also ancillary energy information), so calibration of their time and light response is mandatory.

Absolute timing of events will be important for tracking the time structure of the burst. We expect that some ~ 0.1 fraction of a drift time ($< \text{ms}$) will be sufficient for sensitivity to interesting physics signatures which vary in time. Therefore calibration of absolute timing response will be of value.

Understanding of backgrounds is also critical for reconstruction of low energy events, and for setting detector requirements. Small single-hit blips from ^{39}Ar or other impurities may fake de-excitation gammas and also affect triggering. Backgrounds may be especially important for photon detectors. Understanding of detector response to radiological backgrounds will therefore also be of value.

Potential calibration sources in this energy range include Michel electrons (studied in MicroBooNE [2]), which have a well known spectrum up to ~ 50 MeV. One can also calibrate using γ , β or neutron sources (both intrinsic and external), which primarily give access to energies less than about 10 MeV. It is more challenging to find “standard candles” between 50 MeV and ~ 100 MeV, beyond cosmic-ray muon energy loss. ProtoDUNE could potentially be a test bed for various calibration strategies. One can imagine also ancillary studies of detector response using detectors such as LArIAT [5], MicroBooNE [6], and SBND [7]. The ultimate calibration would be using a source of neutrinos from pion decay at rest, such as that available at the Spallation Neutron Source [8], which have energies up to 50 MeV with a well-understood spectrum.

1.2.3 Exotic Physics

Nucleon Decay and other exotic physics calibration needs are comparable to the LBL program as listed in Section 1.2.1. Signal channels for light dark matter and sterile neutrino searches will be neutral current interactions which are background to the LBL physics program. The nucleon decay group has done studies of detection of the proton decay channel $p^+ \rightarrow K^+ \bar{\nu}$, where the kaon decays to a muon and then a positron [9]. Based on the widths of dE/dx -based metrics of particle identification, qualitatively, we need to calibrate dE/dx across all drift and track orientations at the few percent level or better, which is a similar target of interest as the LBL effort.

1.3 External Measurements Relevant to Calibration

This section presents a summary of available measurements performed with LArTPC detectors that are relevant for the FD calibration strategy. Upcoming measurements from currently operational and future detectors in the Fermilab Short Baseline Neutrino program, and from the ProtoDUNE detectors at CERN are also discussed.

1.3.1 Measurements of detector response model

Energy loss by charged particles traversing liquid argon leads to ionization and scintillation signatures which are eventually recorded as signals in the detector. Several detector effects impact the propagation of these signals and their energy response in the detector. These effects need to be carefully understood and calibrated. A wide range of calibration measurements for such effects has been performed either with R&D test-stands or neutrino detectors. These measurements, with brief discussions pertaining to their relevance, are presented in this section.

1.3.1.1 Scintillation Light

Light detection plays an important role in the analysis of neutrino interactions with LArTPC detectors. Scintillation light provides essential timing information which complements the slow-drifting ionization signal, and can be used to further improve measurements of calorimetric energy loss and particle-identification. Extensive studies of the properties of scintillation light in LAr have been performed with numerous experiments, with significant contributions to knowledge in this subject coming from dark matter as well as dedicated test-stand experiments such as those performed at Fermilab's Proton Assembly Building (PAB).

External measurements of light quenching due to impurities such as nitrogen [10] and methane [11] are useful in determining absolute light yields and the ratio of prompt to late scintillation light ratios. Measurements of the properties of tetraphenyl butadiene (TPB), used to shift argon scintillation light to the visible spectrum, as well as Rayleigh scattering and ionization-dependent light yields are all important for proper simulation of the light response in LArTPC detectors. In addition to studies that impact the calibration of detector effects, a large amount of work has been and is being performed addressing how light yield, performance, and light collection uniformity impact different photon detection technologies. Examples of such measurements, many of which are performed at Fermilab's PAB facility, can be found in references [12], [13], and [14].

1.3.1.2 Ionization Signal

Many detector effects impact the ionization signals (dQ/dx) ultimately recorded by the TPC wires as shown in this equation [15]:

$$dQ/dx = dE/dx \times \frac{1}{W} \times R \times L \times D \times C \quad (1.1)$$

where dE/dx is the energy lost by the particle initially through ionization over a distance dx , W is the energy required to free an electron, R is the recombination factor of electrons with Ar^+ ions, L is the drift lifetime of electrons, D is electron diffusion constant, and C is the calibration of electronics response. The significant impact of these effects is in large part due to the slow drift of ionization electrons in the TPC, of order $\mathcal{O}(1)$ mm/ μs . Detector effects impact ionization electron signals both by quenching the total ionization charge, as well as by producing local variations in detector response. These in turn lead to relative and absolute energy scale variations which impact energy resolution and bias respectively. Careful calibration of these effects can significantly improve the energy resolution and particle identification performance which are essential in order to achieve DUNE's physics goals.

The major effects which impact detector response to ionization energy loss are listed below, together with relevant measurements of these effects.

1. **Ion Recombination** Ionization electrons in the vicinity of positive argon ions can recombine, quenching the TPC signal. This detector effect is dependent on the concentration of e^- -Ar ion pairs produced and the time such pairs spend in close proximity. The first is determined by the local dE/dx energy loss, and the second by the strength of the electric field. Recombination quenches ionization signals by $\sim 50\%$, causing one of the most significant biases in collected signals. Measurements of ion recombination with stopping muons and protons of energy ranges relevant to GeV ν -Ar interactions have been performed by the ICARUS [16] and ArgoNeuT [15] experiments. These measurements are performed in a range of dE/dx which spans from 2 to 25 MeV cm $^{-1}$, at field strengths in the 0.2 to 0.5 kV cm $^{-1}$ range. The models used for these two measurements differ in parametrization, but lead to very similar results with larger differences or order 5% above 10 MeV cm $^{-1}$ of ionization energy loss.

2. **Quenching by Impurities** Impurities such as H_2O and O_2 can absorb drifting electrons quenching ionization signals as they drift towards the readout wire-planes. The impact of quenching by impurities is parametrized as an exponential quenching probability in function of the drift time, referred to as the electron lifetime. The ICARUS [17] and MicroBooNE [18] detectors have measured electron lifetime values which span from one to tens of ms. Few-ms lifetimes lead to 10 to 40% e^- quenching over meter-scale drift distances, causing significant drift-distance dependent variations in the detector's energy response, and must therefore be carefully calibrated.

3. **Electron diffusion** Electron clouds diffuse as they drift towards the anode. This diffusion

effect is typically separated into a longitudinal component, in the E field direction, and an orthogonal transverse component. For fields of $\mathcal{O}(100 \text{ V cm}^{-1})$ and meter-long drift-distances, 1 to 2 mm diffusion is expected. Measurements have been performed by a dedicated experiment at Brookhaven in a wide range of configurations [19] and the 3 ton ICARUS prototype [19]. Knowledge of diffusion effects helps understand the intrinsic position and timing resolution of ionization signals, which in turn informs detector optimization parameters such as wire spacing and signal shaping. Diffusion effects can also lead to percent-level calibration variations in the drift-coordinate. Finally, preliminary simulations utilizing the DUNE 35 ton prototype geometry demonstrate that detailed analysis of the collection plane signal shape of MIP muon tracks can provide information about the event time, commonly called t_0 [20].

4. **Space Charge Effect** Positive ions, which drift at speeds 1×10^{-3} times smaller than electrons, can build up in a TPC leading to localized variations of the electric field. These in turn impact the drift velocity both in magnitude and direction, distorting the image of ionization electrons recorded by the wires. Additionally, the variation in electric field strength impacts ion recombination, and thus the calorimetry of ionization signals. Turbulence in the argon flow can further complicate the impact of space-charge, requiring in-situ measurements for proper calibration. The magnitude of space-charge effects strongly depends on the overall rate of energy deposition in the TPC. Surface detectors, with a high cosmic ray rate, can expect local variations in calorimetric response of order 2 to 3%. The MicroBooNE detector is performing the first measurement of SCE using cosmic-ray muons and a laser calibration signals to produce maps of electric field distortions. Preliminary results and simulations from MicroBooNE [21] suggest field distortions of order 10%, with significant position dependence, and qualitative data-simulation agreement.

1.3.1.3 Calibration Sources

Current and previous LArTPCs have employed some of the calibration sources and systems under consideration for DUNE; later sections describe the capabilities at the DUNE FD, but we summarize here the use of these sources and systems to date. The majority of LArTPC detectors have relied significantly on samples of 100 to 10 GeV particle tracks produced either in neutrino interactions [22] or from cosmic-ray activity to calibrate the detector's response to energy loss. For cosmic-ray muons entering the TPC additional t_0 tagging methods are available, such as tagging of anode-or-cathode piercing tracks [23] or the use of external cosmic-ray taggers, as installed for MicroBooNE and being constructed for SBND and ICARUS [24]. Relying on a diffusion measurement to perform t_0 tagging, as explored by the 35 ton prototype detector, can provide an additional source for calibrations.

Additional calibration systems are being devised actively on ongoing LArTPC experiments. MicroBooNE is developing the use of intrinsic (Ar^{39}) radioactive sources. Laser systems that can produce ionization trails are a valuable option specifically designed to help measure variations in the TPC's electric field. Such a system has been successfully developed [25] and is being currently employed in the MicroBooNE detector for E field measurements.

Of particular importance to calibrations that impact position-dependent variations in the detec-

tor are sources of known drift-time (t_0). PMT-to-TPC matching can be employed to identify the t_0 associated with TPC interactions. Calibration of the detector’s photon detection system (PDS) using an LED system has been developed and documented for the MicroBooNE detector in reference [26].

1.3.2 Measurements of relevant high-level physics quantities

In addition to measurements of specific detector response model parameters, studies that test the models or provide higher level evaluation of detector performance are important for understanding energy resolution and particle identification. A number of such measurements is presented in this section.

1.3.2.1 Particle Identification

Low detection thresholds and accurate particle identification (Particle ID (PID)) are one of the appealing qualities of LArTPC detectors. Studies of PID using calorimetric information have been published by the ArgoNeuT experiment [15]. Novel techniques using deep neural networks have been developed in simulation of MicroBooNE data [27]. Test-beam experiments, such as the LArIAT experiment [5], are ideal for data-driven studies of particle identification. The LArIAT data in particular can perform measurements of secondary re-interactions of pions and protons which impact PID and neutrino interaction classification.

1.3.2.2 Energy Resolution Measurements

The spatial and calorimetric resolution of LArTPCs allow for precise measurements of particle energies and accurate particle identification. For $\mathcal{O}(1 \text{ GeV})$ energy muons which escape the TPC volume, Multiple Coulomb Scattering has been shown [28, 29, 30] to be a viable method to reconstruct the muon momentum with resolutions of order 10 to 20%.

1.3.2.3 Calibration of Detector Response to Electromagnetic Activity

Strong motivation for careful calibrations of EM activity comes from the essential role that electron energy reconstruction plays in DUNE’s oscillation and SNB physics programs. Calibration of a LArTPC’s detector response to electromagnetic (EM) activity introduces several challenges due to the nature of EM energy loss. This is especially true for EM showers in the tens to hundreds of MeV energy range, which directly impact a broad range of DUNE physics measurements. The stochastic nature of bremsstrahlung photon production and 14 cm radiation length in LAr lead, at these energies, to sparse and segmented showers. Energy reconstruction of EM showers relies on the calorimetric measurement of energy deposited in the TPC, and this measurement can be biased by effects such as thresholding (due to small energy deposits) and clustering (due to far-reaching,

isolated energy deposits). Having access to sources of EM energy deposition for in-situ calibrations of such biases is essential. Two such sources have been studied by past measurements:

- **Michel electrons** The well known spectrum of electrons from muon decay at rest makes Michel electrons a powerful source with which to study energy reconstruction for electrons in the tens of MeV. The overlap of this spectrum with the critical energy in LAr makes this sample particularly interesting due to the complex topology which these events exhibit. ICARUS has measured Michel electrons in LAr, studying energy loss by the primary electron [31] with good calorimetric energy resolution. MicroBooNE subsequently has measured Michel electrons studying energy loss both by primary ionization and radiation [2], showing that measuring radiative losses allows to improve the electron energy resolution, while at the same time presenting the reconstruction challenges involved.
- **Neutral Pions** π^0 s provide a valuable calibration source for EM activity. Their primary decay to a pair of photons allows for a data-driven calibration of the photon energy by relying on the π^0 mass value. Studies of EM energy reconstruction utilizing such a sample have been performed by the ICARUS collaboration [32] and are currently underway in MicroBooNE. Studies of π^0 energy reconstruction are also available in a measurement of ν_μ CC π^0 interactions in ArgoNeuT [33].

1.3.3 Future Measurements

A number of currently operational and near-term LArTPC detectors will be producing additional measurements of relevance for detector calibration. The ProtoDUNE-SP [34] and ProtoDUNE-DP will test the technology's scalability and make measurements valuable to particle identification in a 1 kt, 3.6 m drift environment. As MicroBooNE continues to take data, and is joined by the SBND and ICARUS detectors as part of the Short Baseline Neutrino program [7], additional measurements of the above categories will be performed by similar-scale surface detectors. Measurements from the neutrino oscillation and cross-section driven SBN program will specifically focus on calibrations with significant impact on physics analyses and systematics which will deepen the understanding of DUNE calibration sources (Ar^{39}) and systems (laser). MicroBooNE's data will be valuable to explore time-dependant failures or effects due to the long operation running time. In the short term initial studies on EM interactions in LAr [35], of particular importance to DUNE's oscillation physics program, will be expanded.

1.4 Existing Calibration Sources

All dedicated external calibration systems must provide benefits outside of free, copious, and commonly used calibration sources, described in this section. DUNE will use particles from cosmic ray muons (Section 1.4.1), neutrino-induced interactions (Section 1.4.2), argon isotopes (Section 1.4.3) and information from instrumentation data (Section 1.4.4). Cosmic rays and neutrino-induced interactions provide commonly used “standard candles” like electrons from muon and pion decay, and neutral pions, which have characteristic energy spectrums.

1.4.1 Cosmic Rays

Cosmic-ray events will provide the second-largest source of ionization charge in the DUNE FD, after radiological decays. Depending on the triggering strategy, cosmic-ray events may contribute the most to the data volume from the Far Detector. Starting from a predicted rate of four cosmic-ray muons per square meter per day at the 4850’ level at SURF [36], we expect approximately 3 million cosmic-ray particles per year for the four-module FD. A sample of 20,000 cosmic-ray muons was simulated for a 10kt SP module using the MUSUN generator [37] and reconstructed using LArSoft. This simulation draws muon momenta from a pre-computed spectra with full angular and energy dependence given the local rock composition and topography at the SURF laboratory. The energy and angular distributions are given in [36]. The MUSUN generator only simulates single cosmic-ray muons; muon bundles arising from high-energy atmospheric showers are not simulated yet. The rates are uncertain at the level of 20%.

Cosmic rays can provide many critical measurements for DUNE, described in the following subsections. These include detector timing offsets, detector alignment, drift velocity, electron lifetime, relative channel calibrations, absolute gain, electromagnetic response using decay electrons and π^0 . Some events may be useful for some measurements and not others. For example, detector alignment studies require muons that pass over the gaps between anode plane assemblies (APAs), or pierce the APAs or cathode plane assemblies (CPAs), while studying the electron drift and lifetime requires muons that traverse the entire horizontal drift direction between the APAs and CPAs. In the list of possible measurements below, we estimate the daily rate of cosmic-ray muon events that can be used and the requirements used to select these events.

1.4.1.1 Detector Timing Offsets

A measurement of the global time offsets between the TPC wire readout and the photon detectors and external sources of timing information (such as external muon counters), can be made with tracks that cross through the APA volumes. Hits on either side of the APAs drift in opposite directions and thus a constrained fit for a track to line up on both sides of an APA requires the time of the event to be correct. Hits that drift from locations close to the APAs are minimally affected by space charge and other field distortions.

Approximately six non-showering muons are estimated to pierce each APA per day. This number is the nine muons per day crossing a vertical gap, which is estimated in the next section, multiplied by $(2.5\text{ m})/(3.6\text{ m})$, the ratio of the width of an APA to the drift distance. Timing offsets can therefore be measured in under a week on an APA by APA basis, and a global timing offset with less than a day's worth of data.

1.4.1.2 Detector Alignment

The 150 APAs in a SP module are expected to be rigid bodies that are assembled to precise mechanical tolerances. The requirements for physics analyses however often exceed mechanical tolerances that can be achieved, especially after cool down. Straight tracks that cross from the volume of liquid argon that is read out by one APA into the volume read out by another APA give, by steps in their apparent positions and angles, constraints on the relative positions and angles of the APAs as they are situated in the detector. A full alignment campaign using cosmic rays will find the minimum of a χ^2 function that depends on the measured track segments, positions and angles of the APAs and CPA panels, and includes any external constraints such as mechanical surveys, along with realistic uncertainties. Examples of cosmic-ray alignment campaigns can be found from ATLAS [38, 39], CMS [40], ALICE [41]. In the following discussion, the y axis is vertical, the x axis points along the electric field, and z points approximately along the beam direction.

Given experience from the 35 ton prototype, we predict that the precision on the width of a vertical gap between two neighboring APAs is

$$\sigma_{\Delta z} \approx \frac{1.79 \times 10^{-1} \text{ cm}}{\sqrt{N_{\text{tracks}}}}, \quad (1.2)$$

where N_{tracks} is the number of cosmic-ray muon tracks used to make the measurement, and the precision on offsets in the APA positions along the drift direction (aplanar steps) is

$$\sigma_{\Delta x} \approx \frac{5.83 \times 10^{-2} \text{ cm}}{\sqrt{N_{\text{tracks}}}}. \quad (1.3)$$

Naively taking the top half of an APA as a separate measurement from the bottom half and using these precisions to estimate angular resolutions. We thus estimate

$$\sigma \left(\frac{d\Delta z}{dy} \right) \approx \frac{\sqrt{2}\sigma_{\Delta z}(N_{\text{tracks}}/2)}{3 \text{ m}} \approx \frac{1.19 \times 10^{-3}}{\sqrt{N_{\text{tracks}}}} \quad (1.4)$$

and

$$\sigma \left(\frac{d\Delta x}{dy} \right) \approx \frac{\sqrt{2}\sigma_{\Delta x}(N_{\text{tracks}}/2)}{3 \text{ m}} \approx \frac{3.89 \times 10^{-4}}{\sqrt{N_{\text{tracks}}}}. \quad (1.5)$$

The numbers of tracks available to make these measurements depends on the energies, positions, and angles required. The energy of muons is required to be less than 485 GeV, the critical energy in LAr, above which bremsstrahlung and pair production dominate the energy losses over ionization. Tracks that have too many electromagnetic showers along their lengths cannot be used

for alignment, though analyses that use track sections that are locally straight might be able to recover a fraction of these. We require that at least 20 collection-plane wires are hit by a track on either side of a vertical gap, providing enough space points to measure the parts of the track on either side of the gap. Saturation of the analog digital converter (ADC) is an issue for some measurements but should affect alignment studies less than lifetime and signal strength calibrations, so the geometrical requirement is currently estimated to be sufficient. Given the full simulation and these requirements, approximately nine muons that can be used for alignment pass through the argon over a vertical gap every day. Horizontal gaps between APAs that are stacked vertically are shorter, but given the dominantly vertical direction of the incident muons are easier to hit per unit area. We estimate that ten muons per day pass through a horizontal gap and can be used for alignment.

The cathode planes provide additional alignment tasks that can be addressed with cosmic rays. Because there are six cathode plane panels per APA, there are more alignment parameters to consider. Similarly to the ICARUS experience, the volume on both sides of the cathode planes is active, and charge drifts in opposite directions on the sides of the cathode. Thus, if a cathode plane element is displaced in x , a track that pierces it will appear to extend beyond the physical location. We assume the same rate of cosmic-ray muons piercing the cathode planes per unit area as for the APA planes, which means one muon per day per cathode-plane panel is expected. A full alignment with 1 m^2 pixels of the ICARUS cathode took roughly six months of data, and it is reasonable to expect a similar amount of time needed to fully align the cathode panels of DUNE.

One of the main drivers of precise alignment is to be able to use multiple scattering in order to measure muon momentum for muons that escape the detector before stopping. This analysis has been performed by ICARUS [29] and by MicroBooNE [30]. Residual uncertainties in the cathode plane flatness were the limiting systematic uncertainties in the ICARUS measurement.

1.4.1.3 Drift Velocity and TPC Size

Tracks that pierce both an anode plane and a cathode plane in DUNE are particularly valuable. The difference in arrival times of the drifting charge gives the total drift distance divided by the drift velocity, assuming one of these quantities gives a measurement of the other.

1.4.1.4 Electron Lifetime

Tracks that leave ionization at a variety of different distances from the anode provide a sample with which to measure the electron lifetime. Two similar methods have been used. In the first, track charge deposits dQ/dx are measured, the highest and the lowest are ignored because the tail of the Landau offers less information than the core, and an exponential is fit on a track-by-track basis. The track-by-track electron lifetime is then averaged over many such tracks (the reciprocals are in fact averaged to help remove biases due to asymmetric uncertainties). In the second method, a single exponential is fit to the sum of the measured dQ/dx values for many tracks. Examples of these methods can be found from ICARUS [17], MicroBooNE [18], as well as in the 35 ton

2 prototype and the LArIAT detectors

3 references for 35t is "M. Thiesse, Ph.D. Thesis, University of Sheffield, 2018)" and LArIAT?

4 . Extrapolating from the ICARUS precision on $\lambda = 1/\tau$, we expect that each cathode-anode
5 piercing track will provide a $\pm 30\%$ measurement of the lifetime at a lifetime of 3 ms.

6 If one requires tracks to pierce both an anode plane and a cathode plane and have an energy
7 between 20 GeV and 400 GeV in order to be straight and non-showering, then the rate is five per
8 day per drift volume on one side of an APA. If one further requires that the muon pierce one of
9 the six cathode panels directly opposite to the APA it pierced, then the rate falls to 1 per day.
10 ADC saturation is not a concern for tracks that traverse the entire drift length.

11 1.4.1.5 Relative Channel Calibration

12 Channel-to-channel gain variations can be tested with large samples of cosmic-ray muons. The
13 rate at which a single collection-plane channel records useful data from cosmic-ray muons is very
14 similar to that for the vertical gaps between APAs, or roughly ten per day. In this case, ADC
15 saturation is a concern, but traversing forty collection-plane wires in the 6 m height as per the
16 angular requirement for alignment should keep the hits from saturating the ADCs.

17 Nonetheless, a comparison of the gains of faraway channels requires averaging over a large ensemble
18 of cosmic-ray muons, as the muons will have different energies and thus different dE/dx values, and
19 given their dominant vertical directions, each will hit only a portion of an APA. A high-precision
20 calibration of each channel's relative gain will likely take on the order of months, depending on
21 the track-to-track variation in measured dQ/dx values which affects the rate of convergence of the
22 average.

23 1.4.1.6 Absolute Gain Calibration with Minimum Ionizing Particles

24 A measurement of the Minimum Ionizing Particle (MIP) scale in the DUNE FD will be more
25 challenging, as the dE/dx distribution depends on the energies of the incident muons. With a
26 model of the energies, one can find the distribution of dQ/dx values and fit it with a floating
27 global gain value and uncertainties in the parent energy distribution to obtain a global scale. This
28 method is subject to systematic uncertainties arising from the energy scale of the incident muons.

29 1.4.1.7 Electron Response Calibration from Michel Electrons

30 Stopping μ^+ particles will produce Michel electrons with a known energy spectrum which can be
31 used to calibrate the response of the detector. An example analysis of Michel electron reconstruc-
32 tion is available from MicroBooNE [2]. This analysis is sensitive to the collection of energy de-
33

2 posited by bremsstrahlung photons which Compton-scatter a short distance away from the Michel
 3 electron, and is useful in tuning up reconstruction as well as the simulation. Approximately 30
 4 muons per day are expected to stop in a 10 kt module.

5 **1.4.1.8 Electromagnetic Energy Scale from π^0 Decays**

6 An estimate of the rate at which cosmic-ray muons produce π^0 s is of the order of one per 1000
 7 cosmic rays. The ICARUS experiment performed an analysis of 212 candidate π^0 decays from the
 8 2001 Pavia surface test run [32].

9 **1.4.1.9 Limitations**

10 As described in Refs. [38, 39], alignment of detectors using only cosmic-ray muons leaves some
 11 combinations of uncertain parameters only loosely constrained. These are labeled “weak” directions
 12 in the citations above. While the DUNE Far Detector geometry is significantly different from
 13 a collider detector, similar weak directions will appear in the cosmic-ray alignment campaign.
 14 Distortions of the detector that preserve the gap widths and do not shift the APAs in x near the
 15 gaps relative to one another will be difficult to measure with cosmic rays. These distortions include
 16 global shifts and rotations in the locations of all detector elements, and crumpling modes where
 17 the edges of the APAs hold together but angles are slightly different from nominal. An example
 18 of such a distortion is shown in Figure 1.3.

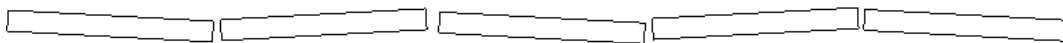


Figure 1.3: An example of a distortion that may be difficult to detect with cosmic rays. The APA frames are shown as rotated rectangles, as viewed from the top.

fig:apacurtainalign

19 There is a global degeneracy between the drift velocity and the drift distance scale in the FD, as
 20 measured with cosmic-ray muons.

21 The uncertainty in the energy spectrum of cosmic-ray muons is a limitation on the global MIP
 22 calibration using these events.

23 Some of the measurements described above, such as the channel-to-channel gain uniformity and
 24 the cathode panel alignment, are estimated to take months of data. We will initially assume that
 25 the calibration parameters are constant and average over the data as it comes in, and only after
 26 larger data samples have been accumulated can more differential measurements be made, such as
 27 constraining time dependence of channel gains and spatial dependence of the electron lifetime.

28 **1.4.1.10 Remaining Studies**

29 Each of the analyses described here requires a full effort to carry to completion with data. Estimates
 1 of sensitivity using simulated data can be used to estimate the levels of precision expected as

functions of time.

The remaining studies for calibration for the TDR related to cosmic ray samples is:

- Quantify what can be achieved for electron lifetime measurements and the overall energy scale calibration from cosmic rays in terms of spatial and temporal granularity.
- Determine what weakly constrained misalignment modes may be important to understand for the physics case. It is expected that combinations of information from cosmic-ray events with other calibration sources (laser-based, neutrino-induced events, and dedicated muon systems) will reduce the total uncertainties, especially for alignment modes which are weakly constrained due to cosmic ray direction.

1.4.2 Neutrino-induced interactions

Beam and atmospheric neutrinos and antineutrinos will provide interactions useful for certain calibrations of the FD. Both sources of neutrinos will produce CC and NC events, where CC interactions will produce a muon or an electron in the event. Table 1.1 summarizes event rates from different neutrino sources. Neutrinos (or antineutrinos) will produce muons outside and inside the detector that can be tagged as partly or fully contained events. Fully contained events provide more information since the total energy (and the total muon energy) can be reconstructed from the muon range and dE/dx .

Table 1.1: Atmospheric [3] and beam neutrino and antineutrino event rates per year in 40 kt fiducial mass of the FD. The beam-rock interaction rate is for the front (beam direction) face of the detector module only; additional interactions will occur along the side.

Event type	Rate/year/40 kt
Fully contained atmospheric e -like	1.6×10^3
Fully contained atmospheric μ -like	2.4×10^3
Partly contained atmospheric μ -like	7.9×10^2
CC or NC atmospheric π^0	300
CC or NC atmospheric K^+	20
Beam induced, rock [42] μ -like	$2.8 - 5.6 \times 10^3$
Beam induced, LAr (signal) μ -like	2.8×10^3

1.4.2.1 Possible Measurements

Although cosmic-ray muons have much higher event rates compared to atmospheric or beam neutrinos, CC events from neutrino interactions have a few advantages. Beam events will complement cosmic-ray muon calibration, in particular at near-horizontal directions ($\cos \theta < 0.3$) where cosmic-ray muons are absent. Neutrino-induced muons will help with testing the APA alignment. How-

ever, only muons with relatively high energy will provide accurate measurements since low-energy muons may undergo multiple coulomb scattering.

Both partially and fully contained muon events will provide a sample of electrons from muon decay (for electron ID and shower calibration). In addition, negative muon capture events, which emit protons and neutrons will be a valuable sample. This topology is relevant to various rare event searches, like nucleon decay, which rely on separating positive kaons from a sub-sample of negative kaons. Beam-induced events will also provide a small but valuable π^0 sample for energy scale.

Beam-induced events may also be used for reconstruction validation in certain circumstances. A ν_μ or ν_e CC neutrino event tagged by a clear identification of a muon or an electron (via a shower) will allow testing for lepton identification. There should be no other lepton emerging from the primary vertex in such events, so any additional lepton found by the reconstruction (not coming from a secondary hadronic decay) would indicate reconstruction pathologies. Neutrino events will have more predictable outcomes and topologies compared to higher energy cosmic-ray muon events, and have a higher probability of producing low-energy hadrons. Although some of these events are signal for the long-baseline program and will not be used directly for calibration parameter measurements, one can test the particle identification using beam events for rare event searches, e.g., nucleon decay or neutron-antineutron oscillations.

1.4.2.2 Limitations

The main limitation for using neutrino-induced events is their low rates. Due to this, their application for calibration is quite limited. While they may provide supplementary information on energy calibration (dE/dx and electromagnetic showers) and can be used for particle ID reconstruction tests, any calibration required on a daily basis is impossible with these events. It will also be difficult to get accurate results for individual TPCs within the FD with these events.

We also note that the beam from LBNF at Fermilab will probably be ready a year or two after the commissioning of the first detector module. Hence beam neutrinos may not contribute to the first module calibration at the beginning of running.

1.4.2.3 Remaining Studies

The majority of work related to neutrino-induced interactions has occurred in connection with atmospheric neutrinos for nucleon decay searches. Due to the statistical limitation of these samples, it is expected that they will be used as cross checks more than

The remaining studies for calibration for the TDR related to neutrino-induced samples is:

- Quantify the impact on energy scale from π^0 sources, and the relative importance of electromagnetic shower photons below pair production threshold (shared with cosmic rays, long baseline studies)

- Determine what misalignment modes (shared with cosmic ray alignment studies and dedicated muon system, discussed in Section [?] and Section [?] respectively) are resolved with neutrino induced events.

1.4.3 Argon 39

The reconstructed energy spectrum of ^{39}Ar beta decays can be used to perform a variety of in-situ and ex-situ measurements of detector effects relevant for particle reconstruction in the DUNE Far Detector. The ^{39}Ar beta decay rate in natural (atmospheric) argon is about 1 Bq kg^{-1} , so $O(50\text{k})$ ^{39}Ar beta decays are expected in a single 5 ms event readout in an entire 10 kt detector module. The ^{39}Ar beta decay cut-off energy is 565 keV which is close to the energy deposited on a single wire by a MIP. Another useful feature of ^{39}Ar beta decays is that they are uniform in the drift direction.

1.4.3.1 Possible Measurements

Given that the large number of ^{39}Ar beta decays are present through out the volume of the detector, this method allows for a fine-grained (spatially and temporally) electron lifetime measurement in the FD. It can also provide other necessary calibrations, such as measurements of wire-to-wire response variations and diffusion measurements using the signal shapes associated with the beta decays, and could serve as an online monitor of electric field distortions in the detector by looking at the relative number of decays in the detector near the edges of the LArTPC. The viability of this method has already been demonstrated with MicroBooNE data (results expected to be released publicly sometime later this year), both for MicroBooNE and a projection to conservative operating conditions of the Far Detector.

Using the fact that the ^{39}Ar beta decays are uniformly distributed in the drift direction, one is able to precisely determine the expected reconstructed energy spectrum for a given set of detector response parameters. This can be done independently of using timing information (e.g. from prompt scintillation light). As an example, one can use the reconstructed ^{39}Ar beta decay energy spectrum to constrain primary detector response parameters such as the electron lifetime and recombination simultaneously. Figure 1.4 illustrates the different possible reconstructed ^{39}Ar beta decay electron energy spectra one might see after correcting for all other detector effects except for electron lifetime, for ^{39}Ar beta decays occurring in the SP module. Also shown in Figure 1.4 is the impact of varying the true recombination model from the one assumed in energy reconstruction of the ^{39}Ar beta decay electron, with infinite electron lifetime. The impact on the reconstructed energy spectrum is very different for the two detector effects, allowing for simultaneous determination of both quantities.

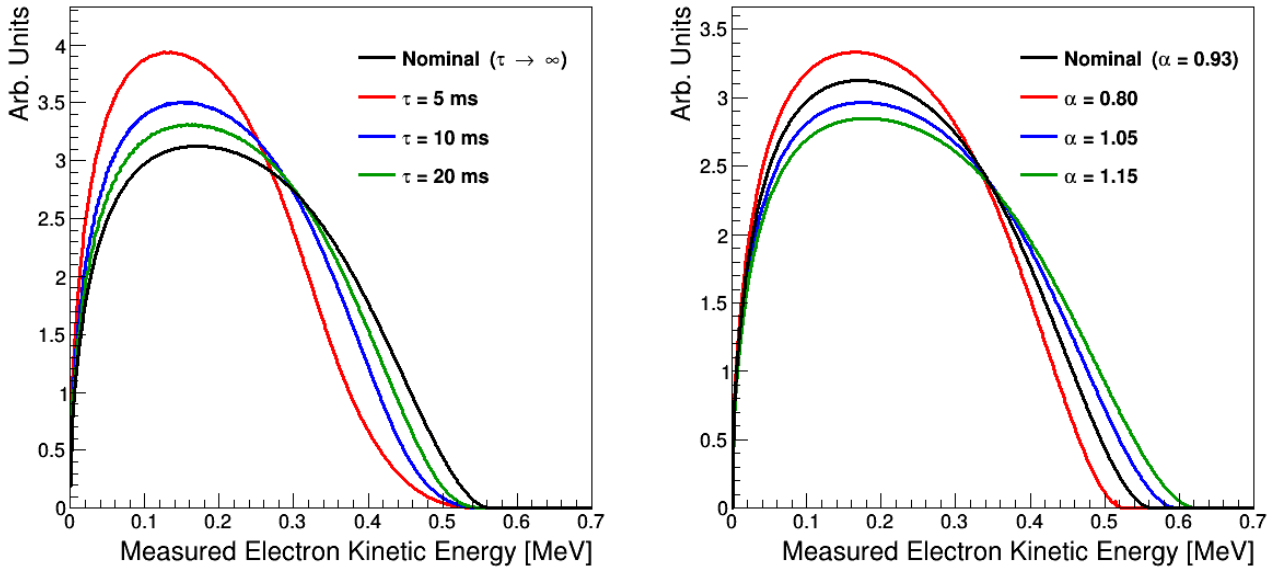


Figure 1.4: Illustration of the impact of different detector effects on the reconstructed ^{39}Ar beta decay electron energy spectrum for decays observed in the SP module. On the left are examples of the reconstructed energy spectrum for various different electron lifetimes, as well as the nominal ^{39}Ar beta decay spectrum (corresponding to an infinite electron lifetime). On the right are examples of the reconstructed energy spectrum when the true recombination model is different from the one assumed in energy reconstruction (varying the α parameter of the modified Box model, $\mathcal{R} = \ln(\alpha + \xi)/\xi$, where $\xi = \beta \frac{dE}{dx} / \rho E_{\text{drift}}$ and with fixed $\beta = 0.212$) and the electron lifetime is infinite. All curves have been normalized to unit area.

fig:ar39

1.4.3.2 Limitations

There are several factors that impact the observed charge spectrum from ^{39}Ar beta decays such as electronics noise, electron lifetime and recombination fluctuations. The effect of electron lifetime is more pronounced in dual phase due to the longer drift distance requiring the measurement be carried out more precisely. Also for this method to work, noise level must not be too high (requires less than $1000\text{ e}^- \text{ ENC}$) and a precision noise measurement is required. Another limitation of this method is that ^{39}Ar beta decays closer to the cathode will be more likely to be below threshold (and thus undetected) in comparison to ones closer to the anode. This can impact the interpretation of the result. Extrapolating to regions closer to the cathode requires making the assumption that the electron lifetime is constant as a function of the drift coordinate, which may not be the case. In the case that there is variation in x , one could make use of an auxiliary measurement using t_0 -tagged cosmic muon tracks to determine the dependence of electron lifetime on x . However, this would require integrating over a much larger period of time in order to obtain the appropriate level of statistics. External radiological sources may be able to make this measurement in limited parts of the detector more quickly, though this requires further study.

One important consideration is whether or not the DUNE Far Detector DAQ system can provide the necessary rate and type of data in order to successfully carry out this calibration at the desired frequency and level of spatial precision. From studies at MicroBooNE, an estimate of the number of decays necessary to carry out a percent-level calibration of electron lifetime is $O(250\text{k})$. However, one must also allow for the electron lifetime to spatially vary throughout the entire 10 kt module; it is not clear how much variation one should expect in a detector of this size. For a granularity of one measurement in every m^2 drift volume once per day, a roughly 1 Hz for minimum-bias event trigger rate is needed; this is comparable to other LArTPC detectors that are currently operating. The data rate would be roughly 4 GB s^{-1} for an entire 10 kt module without zero suppression.

Note that the DAQ rates estimated previously do not take into account the need to save the required amount of data on the induction planes, which will have higher noise levels. It might be necessary to save data from many induction plane wires for a candidate ^{39}Ar beta decay found on a single collection plane wire, leading to a much higher data rate (a factor of $O(100)$ higher). One can get around this requirement by making the electron lifetime measurement strictly in the z direction (by far the longest dimension of the detector, and thus the most interesting to probe for spatial variations of electron lifetime), or by introducing a tighter requirement on the reconstructed charge threshold for the induction planes.

1.4.3.3 Remaining Studies

Currently, the plan is to study this calibration technique in more detail first with data from ProtoDUNE, well in advance of first operations with the FD, to gain lessons learned and understand the challenges for DUNE.

1.4.4 Instrumentation and Monitoring Data

Several instrumentation and detector monitoring devices will provide valuable information for calibrations. The cryogenics instrumentation and detector monitoring effort for DUNE is centrally led by the Cryogenics Instrumentation and Slow Controls (CISC) consortium. The instrumentation devices include liquid argon temperature monitors, LAr purity monitors, gaseous argon analyzers, and cryogenic (cold) and inspection (warm) cameras. Other instrumentation devices such as drift HV current monitors and external charge injection systems will be useful for calibrations that will be led by the High Voltage and TPC Cold Electronics consortia, respectively. The computational fluid dynamics (CFD) simulations play a key role for calibrations initially in the design of the cryogenics recirculation system, and later for physics studies when the cryogenics instrumentation data is used to validate the simulations. This section provides a brief description of possible measurements with various instrumentation devices and of the detector monitoring data that will be useful for calibrations.

1.4.4.1 Possible Measurements

Electro-negative contaminants such as oxygen and water in the LAr can absorb signal electrons created from the ionization of argon atoms. The gas analyzers can be used for measuring these contaminants in the liquid. There is a plan to deploy a gas analyzer system for DUNE that will be capable of taking measurements at multiple points around the cryogenics system. In addition to gas analyzers, purity monitors provide quick measurements of LAr purity by measuring electron lifetime (via the anode-to-cathode charge ratio) in a small space, typically less than a meter. The purity monitor measurements are especially useful during detector commissioning and initial operations when cosmic-ray data will not be available to perform more detailed studies. Electron lifetime correction is an important step in calorimetric reconstruction and can impact many other parameters such as electron recombination and track reconstruction. There is a plan to deploy three purity monitors inside the cryostat and some in the inline filters of the argon purification system.

Several thermometers, both individual sensors and vertical temperature gradient monitors (both static and movable), will be installed throughout the volume of the cryostat to provide LAr temperature measurements with a precision goal of 5 mK. The biggest impact of LAr temperature is on the electron drift velocity through the drift coordinate, which in turn affects the fiducial volume. Drift velocity can also impact measurements like electron diffusion. Both temperature and purity monitor data will be critical for validating the LAr flow model. Validation of the fluid-flow model using instrumentation data will give confidence in its projections regarding the impact of various liquid flow properties on the physics. In addition to the instrumentation data, the cryogenics system data such as LAr contamination levels, temperatures and various flow parameters will be continuously monitored and recorded, providing additional information for calibrations.

DUNE plans to deploy both cryogenic cameras and inspection cameras. The cryogenic cameras will be used to look for HV activity, especially breakdowns. The inspection cameras will be used to monitor the health of the detector components and to visually diagnose any issues that arise.

Data from both types of cameras will be useful for calibrations to understand any electric field anomalies or unexpected drift field responses. Additionally, to further monitor and diagnose HV issues, installing devices such as current monitors will be useful to diagnose or characterize the field cage (FC). The experience from MicroBooNE using a source meter to continuously monitor pick-off point voltage with respect to the detector ground has helped the collaboration diagnose HV problems. In both SP and DP systems, the failure of a resistor will create a significant, local electric field distortion which will need to be identified. In the DP system, four registers would have to fail to cause a failure across the field cage gap, but even one failure in the SP can have an impact; this may be partially mitigated by modifying the HV.

1.4.4.2 Limitations

While purity monitors have practical advantages in terms of speed of measurement and the ability to measure low electron lifetimes before tracks can be reconstructed, purity monitor measurements are very localized and do not necessarily reflect any purity variations in the cryostat. Also, purity monitors typically measure the effect of the contaminants at a lower electric field. In fields above about 200 V cm^{-1} , the drift field increases the speed of the drift electrons

increases in the field cause increases in drift speed? pls clarify

and this can lead to a different electron-capture cross section on the contaminants for the purity monitor and the drift electrons in the TPC. Additionally, purity monitors have a limited lifetime, making it important to be aware that they will not be able to provide measurements for the entire lifetime of the experiment. To mitigate this, MicroBooNE has developed a nearline purity monitoring system that uses a statistically sufficient sample to make a purity measurement once every few hours using cosmic-ray muons. Developing similar techniques for DUNE will be very useful. The low cosmic-ray rate might be an issue for DUNE, but it may be possible to make less frequent nearline measurements.

The fluid flow within DUNE is a unique challenge and the fluid flow model needs validation. The fluid recirculates on the timescale of 21 days, but there may be fluid exchanges on shorter timescales. The liquid argon flow pattern, if steady state can trap some ions indefinitely causing stable eddies that can significantly impact the space charge distribution.

Need to confirm this number

previous sentence needs work; I cannot parse it

In MicroBooNE the flow pattern is turbulent so this does not occur, but this is not understood yet for DUNE. Temperature monitor data are used to validate the fluid flow model, but achieving the required precision with thermometers is a challenge. The precision will affect the quality of the fluid flow model validation.

The presence of a FC resistor failure will be detectable, however it will not be possible to determine where it has failed spatially from monitoring data. The position must be determined by existing or in-situ calibration systems.

1.4.4.3 Remaining Studies

The remaining studies prior to the TDR are:

- Validation of the fluid flow model using instrumentation data at ProtoDUNE.
- Implementation of a nearline purity monitoring using cosmic rays (as does MicroBooNE) to understand the challenges of implementing such a system in a larger-scale detector.
- Use of current CFD simulations to understand the range of variation for various flow-related parameters (e.g., overall temperature variation in the cryostat, overall impurity variation across the detector module) and propagation of those variations to calibration to understand the impact on physics.
- CFD studies to understand how LAr flow can impact space charge and ion accumulation (both positive and negative ions). This will be especially critical for the DP module design due to the liquid-gas interface, as described in detail in Section 1.5.

1.5 Dual Phase Considerations for Calibration

Some unique features of the DUNE DP module design require special considerations regarding calibration. These features include the single vertical 12 m long drift, gain of the LEMs, ion accumulation at the liquid-gas interface, and the LAr flow pattern. All of these can amplify the nominal space-charge effect expected in the detector module.

While space charge from cosmic rays is expected to be negligible in both SP detector module and DP detector module, other ionization sources such as ^{39}Ar can result in non-negligible E field and spatial distortions. Simulation studies have shown that the space charge from ^{39}Ar is more pronounced for DP especially for spatial distortions (at the 5 cm level with a 2 to 3% impact on dQ/dx via recombination) as shown in Figure 1.5. The LAr flow pattern can amplify space-charge effects as well, which may be significant for dual phase (as well as single phase).

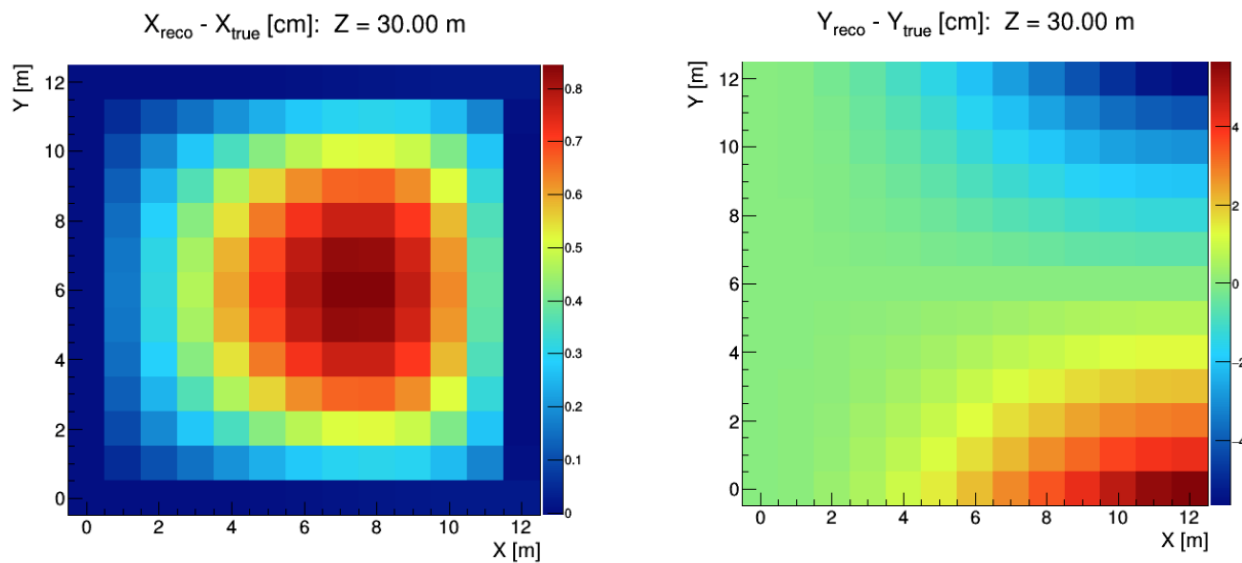


Figure 1.5: Illustration of the simulated effects of space charge on distortions in reconstructed ionization electron cluster positions in the DP detector module. Results are shown for the effect in x (left) and y (right). The distortions in reconstructed ionization-electron cluster position are shown in units of cm and are plotted as a function of the true position in the TPC. Simulation results are shown for a central slice in z . APA corresponds to $x = 0$ and CPA corresponds to $x = 12\text{m}$.

The gain of the LEMs will also need to be calibrated in the DP detector module. Any error in the charge gain in the LEM will directly impact the energy uncertainty for electromagnetic showers. The LEM gain is sensitive to many factors such as the hole size, copper rim offset, board thickness, hole inner surface conductivity, charging effects, and extraction and collection field (gap between electrodes). A gain map of the entire LEM surface will be needed, and if the gain drifts with time, periodic re-mapping of the gain may be needed. Furthermore, it is unclear how the charge and discharge cycles (e.g., due to a 12 m vertical cosmic track) impact the stability of gain. Additionally, a reduced gain can result in much stricter requirements on the electron lifetime.

An additional complication for dual phase involves positive ions collecting above the liquid-gas

3 interface and creating surface interface issues which can lead to significant spatial distortions.
4 If the electron lifetime is poor, it can result in electrons being captured by impurities, forming
5 negative ions that can drift up toward the LEM. If these negative ions (or the electrons stripped
6 off these ions) cannot be extracted into the gas phase by the extraction field, the negative ions
7 will build up at the liquid surface forming non-uniform negative surface charge. This non-uniform
8 negative surface charge will distort the electron drift path; it may also change the extraction field
9 and alter the gain of LEMs in gaseous argon.

10 The size of this effect needs to be understood and possibly calibrated. The ProtoDUNE-DP, given
1 its size, would be an excellent test bench to observe all the effects mentioned in this section. More
2 dedicated studies will be planned in this direction with the ProtoDUNE-DP group.

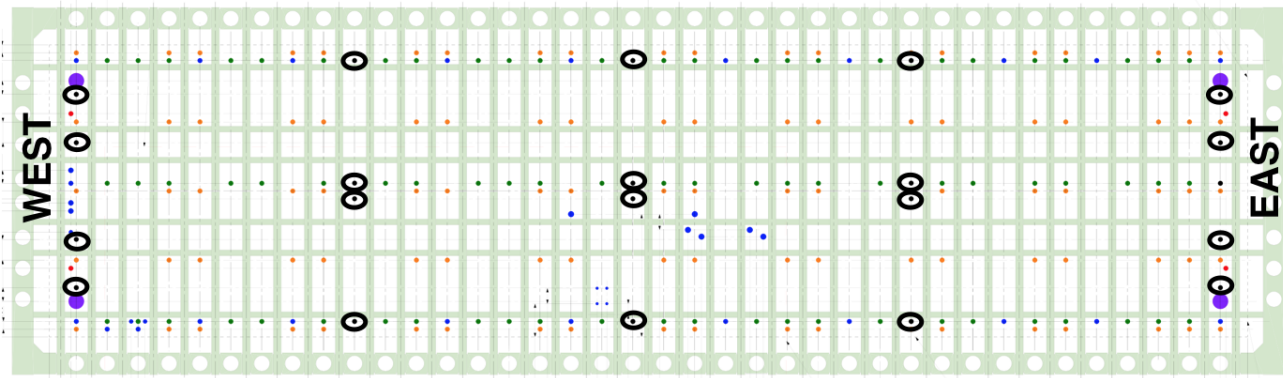


Figure 1.6: Top view of the SP detector module cryostat showing various penetrations. Highlighted in black circles are multi-purpose calibration penetrations. The orange dots are TPC signal cable penetrations. The blue ports are DSS penetrations. The orange ports are TPC signal cable penetrations. The larger purple ports at the four corners of the cryostat are manholes.

fig:ftma

3 1.6 Calibration Systems Under Consideration for DUNE

tsystems

4 This section describes the calibration systems currently under active consideration for the DUNE
 5 detector modules, both single phase and dual phase. As the physics motivation and design con-
 6 siderations for each system are being discussed and reviewed, feedthrough accommodations have
 7 been made for the SP detector module as described in Section 1.6.1.

8 1.6.1 Calibration Penetrations

sec:FTs

9 The current cryostat design for the SP detector module with penetrations for various sub-systems
 10 is shown in Figure 1.6. The penetrations dedicated for calibrations are highlighted in black circles.
 11 The ports on far east and far west are located outside the field cage. The current plan is to
 12 use these penetrations for multiple purposes. For example, the penetrations on the far east and
 13 west will be used both by laser and radioactive source deployment systems. In addition to these
 14 dedicated ports, the Detector Support System (DSS) and cryogenic ports (orange and blue dots
 15 in Figure 1.6, respectively) will also be used as needed to route cables for the single phase photon
 16 detector calibration system. The DSS and cryogenic ports are accommodated with feedthroughs
 17 with a CF63 side flange for this purpose.

18 The placement of these penetrations is largely driven by the ionization track laser and radioactive
 19 source system requirements. The ports that are closer to the center of the cryostat are placed near
 20 the APAs (similarly to what is planned for SBND) to minimize any risks due to the HV discharge.
 21 For the far east and west ports, HV is not an issue as they are located outside the FC and the
 22 penetrations are located near mid-drift to meet radioactive source requirements. Implementation
 23 of the ionization track laser system proposed in Section 1.6.2, requires 20 feedthroughs to cover
 1 the four TPC drift volumes; this arrangement would provide (almost) full volume calibration of
 2 the electric field and associated diagnostics (e.g. HV). The crossing laser tracks are necessary to

3 unambiguously construct the field map.

4 The distance between any two consecutive feedthrough columns in Figure [fig:ftmap](#) 1.6 is assumed to be
5 about 15 m. This is considered reasonable since the experience from the MicroBooNE laser system
6 has shown that tracks will propagate over that detector's full 10 m length. Assuming that the
7 effects of Rayleigh scattering and self-focusing (Kerr effect) do not limit the laser track length, this
8 laser arrangement could illuminate the full volume with crossing track data. It is important to
9 note that at this point in time, a maximum usable track length is unknown and it is not excluded
10 that the full 60 m detector module length could be achieved by the laser system after optimization.

11 The calibration group focused on finalizing the cryostat penetrations for the SP detector module
1 driven by the cryostat design timeline. In the near future, a similar exercise will be done to finalize
2 DP detector module penetrations for calibrations.

1.6.2 Laser Systems

electric field, E field or E-field? We have to decide for entire TP!

The Calibration task force has considered multiple systems that use a laser to extract the electric field map. They fall into two categories: photo-electron and direct ionization of the LAr, both driven by a 266 nm laser system.

The system considered to be the primary reference design uses direct ionization and multiple laser paths, as it has the largest potential benefit as described in Section 1.6.2.1. An ionization-based system has been used in the ARGONTUBE [43], MicroBooNE, CAPTAIN and SBND experiments.

1.6.2.1 Motivation and Possible Measurements

The main purpose of a laser calibration system is to provide a measurement of the electric field in the detector with high statistics. Many useful secondary uses of laser include alignment, stability monitoring, and diagnosing detector failures (e.g., HV). As discussed in earlier sections, several detector parameters such as drift velocity and recombination which ultimately impact the spatial resolution and energy response of the detector have critical dependence on the electric field. Approximately, a 1% distortion in the E field corresponds to a 0.25% effect on dQ/dx . E field distortions can occur globally or locally, and are caused by a variety of effects. Although the space charge due to ionization sources such as cosmic rays or ^{39}Ar is expected to be small, fluid flow pattern make the effect significant in both SP and DP modules. Also, as discussed in Section 1.5, this effect can get further amplified significantly in the DP due to ion accumulation at the liquid-gas interface.

Additionally, other sources in the detector (especially detector imperfections) can cause E-field distortions. For example, CPA misalignment, CPA structural deformations, APA and CPA offsets and deviations from flatness can create localized E-field distortions. Non-uniform resistivity in the voltage dividers that produce the E-field may create a net E-field distortion localized in space, and a failure of a FC resistor will make the distortions time dependent. Each individual E-field distortion may add in quadrature with other effects, and can exceed a 1 to 4% overall E-field distortion. Understanding all these effects require in-situ measurement of E-field for proper calibration. A laser system also has the intrinsic advantage of being immune to recombination, thus eliminating particle-dependent effects.

Assuming multiple, steerable laser entry points as discussed in Section 1.6.1, the ionization-based system can extract the electric field with fewer dependencies compared to other systems. An unambiguous field map requires crossing laser tracks in every relevant voxel² of the detector. If two tracks that enter the same spatial voxel² ($10 \times 10 \times 10\text{cm}^3$ volume) in the detector module, the relative position of the tracks provides an estimate of the local 3D E-field. Assuming a single,

²Finer sampling in certain regions may be desirable, but data acquisition (DAQ) requirements prevent much finer sampling for overall E-field mapping.

3 steerable laser track, the apparent curvature of the track can also be used to assess (more limited)
 4 information about the electric field.

5 Even if the laser is not intense enough to ionize the LAr, electrons may be liberated from material
 6 on the cathode, which provides many useful measurements. The total drift time can be assessed
 7 from laser pulse to readout of charge on the anode. A photo-electron-based calibration system
 8 was used in the T2K gaseous (predominantly Ar), TPCs [44]. Targets placed on the cathode
 9 provided dots and lines that were then imaged by the electronics, and relative distortions of the
 10 surveyed positions could be used. The T2K photo-electron system provided measurements of
 11 adjacent electronics modules' relative timing response, drift velocity with few ns resolution of
 12 870 mm drift distance, electronics gain, transverse diffusion, and an integrated measurement of the
 13 electric field along the drift direction. For DUNE, the system would be similarly used as on T2K to
 14 diagnose electronics or TPC response issues on demand, and provide an integral field measurement
 15 and relative distortions of y , z positions with time, and of either x or drift velocity. Ejection of
 16 photo-electrons from the direct ionization laser system has also been observed.

17 1.6.2.2 Design Considerations

18 For either system, a 266 nm laser would be mounted on the top of the cryostat, and service two
 19 adjacent feedthroughs. A steerable head and fiber interface would be mounted in the feedthrough,
 20 which is coated in a insulator. Two options are under investigation: (1) the FC (but not the
 21 ground plane (GP)) is penetrated, and (2) the FC is not penetrated. In the former case, the
 22 FC penetration has been shown to create a small distortion to the E-field, for the benefit of full
 23 volume E-field mapping. When the FC is not penetrated, the laser shines through the FC tubes,
 24 producing some regions that are not mappable by the laser. Unlike the ports that are inwards of
 25 the cryostat, the lasers through penetrations that are outside the FC on the far east and west side
 26 of the cryostat will not penetrate the field cage. The photo-electron system would include a fiber
 27 and no steering; the necessity of penetrating the FC is unlikely but has not been assessed yet.

28 The current feedthrough penetrations are spaced at a 15 m, a plausible distance for the laser beam
 29 to travel; the maximum distance light would travel would be to the bottom corner of the detector,
 30 approximately 20 m. Direct-ionization tracks have been demonstrated at a maximum possible
 31 distance in MicroBooNE of 10 m. While the Rayleigh scattering of the laser light is about 40 m,
 32 additional optics effects, including self-focusing (Kerr) effects may limit the maximum practical
 33 range.

34 1.6.2.3 Remaining Studies

35 The remaining studies for the laser systems to be done prior to the TDR are:

- 1 • Determine a nominal design for photoelectric targets on the cathode, and whether such
- 2 targets would provide sufficient survey-like information.

- 3 • Determine if the known classes of possible E-field distortions require penetration of the FC
4 (versus reduced sampling from shining between the field cage).
- 5 • Further understand limitations on laser location precision, practical range of propagation
6 due to optics design and Rayleigh scattering.
- 1 • Continue to quantify the range of possible E-field distortions in the DUNE FD to further
2 refine the estimation of overall variation of E-field (both locally and globally) in the detector.

1.6.3 Radioactive Source Deployment System

sec:rs

1.6.3.1 Motivation and Possible Measurements

Radioactive source deployment provides an in-situ source of the electrons and de-excitation products (gamma rays) which are directly relevant of physics signals from supernova neutrino and/or 8B solar neutrinos. Secondary measurements from the source deployment include electro-magnetic (EM) shower characterization for long-baseline ν_e CC events, electron lifetime as a function of detector module vertical position, and help determine radiative components of the decay electron energy spectrum.

1.6.3.2 Design Considerations

In order to observe γ -signals inside the active volume of the LArTPC from a radioactive source deployed outside of the FC, the γ -energy has to be about 10 MeV. For safety, the source would be deployed about 30 cm from the field cage, so the γ -energy would need to travel two attenuation lengths. Such high γ -energies are typically only achieved by thermal neutron capture, which invokes a neutron source surrounded by a large amount of moderator, thus making such an externally deployed (n, γ) source 20 cm to 50 cm in diameter. In [?], a ^{58}Ni (n, γ) source, triggered by an AmBe neutron source, was successfully built, yielding high γ -energies of 9 MeV. DUNE proposes to use a ^{252}Cf or AmLi neutron source with lower neutron energies, that requires less than half of the surrounding moderator, and making the ^{58}Ni (n, γ) source only 20 cm or less in diameter. The multipurpose instrumentation feedthroughs currently planned are sufficient for this, and have an inner diameter of 25 cm.

I don't find citation bib:Triumf:NickelSource (anne)

The activity of the radioactive source is chosen such that no more than one 9 MeV capture γ -event occurs during a single 2.2 ms drift period. This allows one to use the arrival time of the measured light as t_0 and then measure the average drift time of the corresponding charge signal(s). The resulting drift velocity in turn yields the electric field strength, averaged over the variations encountered during the drifting of the charge(s). This can be repeated for each single 9 MeV capture γ -event that occurs during a 2.2 ms drift period and where visible γ -energy is deposited inside the active volume of the TPC. This restricts the maximally permissible rate of 9 MeV capture γ -events occurring inside the radioactive source to be less than 1 kHz, given a spill-in efficiency into the active LAr of less than 10%.

A successfully employed multipurpose fish-line calibration system []

need to add reference: Double Chooz: NEAR DETECTOR TECHNICAL DESIGN REPORT EDMS ID:I-028812 ; DocDB ID: 3403-V5 Pages 198 - 223 (Anne can't find proper ref for this)

for the Double Chooz reactor neutrino experiment will become available for DUNE after the

decommissioning of Double Chooz in 2018. The system can be easily refitted for use in DUNE. The system would be deployed using the multipurpose calibration feedthroughs located near mid-drift (in each TPC module) on the east and west ends of the cryostat. The sources would be deployed outside the FC within the cryostat to avoid regions with a high electric field. Also, if the source is in close proximity of an APA wire frame, lower energetic radiological backgrounds become problematic as the source light and charge yield is reduced exponentially with distance. The sources are removable and stored outside the cryostat.

The commissioning plan for the source deployment system will include a dummy source deployment (within two months of the commissioning) followed by first real source deployment (within three to four months of the commissioning) and a second real source deployment (within six months of the commissioning). In terms of the run plan, assuming stable detector conditions, a radioactive source will be deployed every half year. Ideally, a deployment before a run period and after the run period is desired so that at least two data points are available for calibration. This also provides a check if the state of the system has changed before and after the physics data run. If stability fluctuates for any reason (e.g., electronic response changes over time) at a particular location, one would want to deploy the source at that location once a month, or more often, depending on how bad the stability is. It is expected that it will take a few hours (e.g., eight hours) to deploy the system at one feedthrough location and a full radioactive source calibration campaign might take at least a week.

1.6.3.3 Remaining Studies

Some ongoing and remaining studies for the radioactive source calibration include:

- Continued development of new geometry tools for source deployment system in simulation along with improving the implementation of the details of the DUNE geometry
- Continued development of simulation tools to understand impact from various radiological contaminants on detector response;
- Studies to suppress radiological backgrounds for the calibration source;
- Simulation studies to understand data and trigger rates;
- A test of the Double Chooz fish-line deployment system with a LAr mock-up column in the high bay lab at South Dakota School of Mines and Technology.
- ProtoDUNE data will provide the first cross check as to how the simulated light and charge yields compare with real data.
- A radioactive source deployment in a potential phase 2 of ProtoDUNE could be envisaged to demonstrate proof of principle of the radioactive source deployment. However, studies need to be performed to first understand how cosmic rays can be vetoed enough such that they would not impact the test deployment of a radioactive source in a surface LArTPC.

1.6.4 External Neutron Source

In a LArTPC, for a fixed amount of ionization deposited at a point in the detector, the amount of charge produced and collected depends on several factors such as argon purity, electron lifetime, noise, and strength of E-field. Given these factors, it is highly desirable to have a “standard candle” energy deposition of known energy that can be detected throughout the volume. Such a standard deposition would reveal variations in the local electron collection efficiency, especially if the source could be triggered such that the t_0 of the interaction was known. An external neutron generator system would be a triggered, known charge source.

1.6.4.1 Motivation and Possible Measurements

The neutron generator system takes advantage of a remarkable property of argon – the near transparency to neutrons with an energy near 57 keV due to an anti-resonance in the cross section caused by the destructive interference between two high-level states of the ^{40}Ar nucleus. As shown in Figure 1.7, this cross section is about 10 keV wide, and at the bottom the cross section of 1.6×10^{-4} implies an elastic scattering length of over 2000 m. Thus to neutrons of this energy the DUNE LArTPC is essentially transparent, and if injected from the top of the detector, would reach every part of the active volume. Of course, natural argon has three major isotopes: ^{36}Ar (0.3336%), ^{38}Ar (0.0834%), and ^{40}Ar (99.6035%) each with a slightly different anti-resonance.

(NOTE: PUT IN EFFECTIVE CROSS SECTION)

NOTE: PUT IN PLOTS FOR ELASTIC

Resolution of plots too bad and labels/titles not readable; get updated plots

I don't find cit for ref:ENDF -anne

Those that do scatter lose energy, leave the anti-resonance (where the scattering length is about 70 cm), quickly slow down and are captured. Each capture releases exactly the binding energy difference between ^{40}Ar and ^{41}Ar , about 6.1 MeV in the form of gamma rays. As will be described below, by using a *DD Generator*³, a triggered pulse of neutrons can be generated outside the TPC, then injected via a dedicated hole in the insulation into the LAr, where it spreads through the entire volume to produce “standard candle” 6.1 MeV energy depositions. Using this method, the calibration procedure would be quick (likely less than 30 minutes).

A relevant question is what fraction of neutrons slowing down from higher energy will fall into the anti-resonance. Figure 1.8 shows an expanded view of the total ^{40}Ar cross section in the range 10 to 200 keV. Since the average energy loss of a neutron elastically scattering off a ^{40}Ar nucleus is 4.8%, in the region of the anti-resonance the average energy loss per scatter is about 3 keV.

³DD stands for "Deuterium-Deuterium"

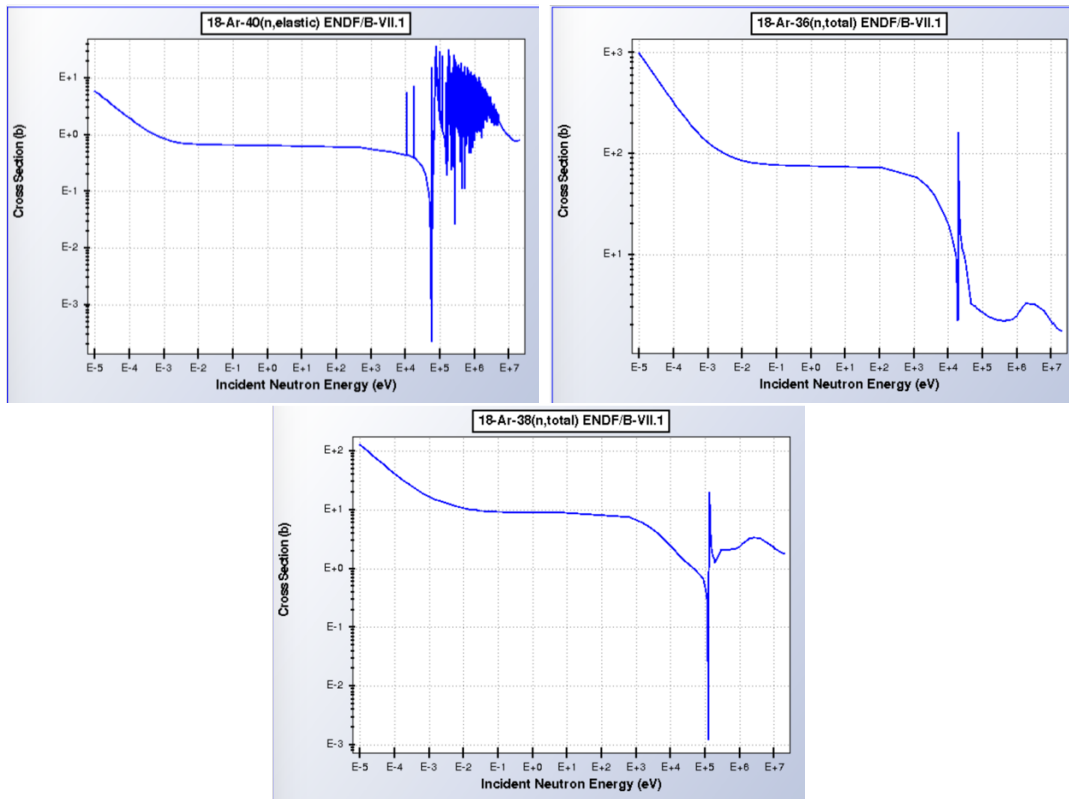


Figure 1.7: Elastic scattering cross sections on ^{40}Ar (top left), ^{36}Ar (top right), and ^{38}Ar (bottom). From ENDF/B-VII.1 [?]. The large anti-resonance at 57 keV in ^{40}Ar can be clearly seen.

fig:Arxs

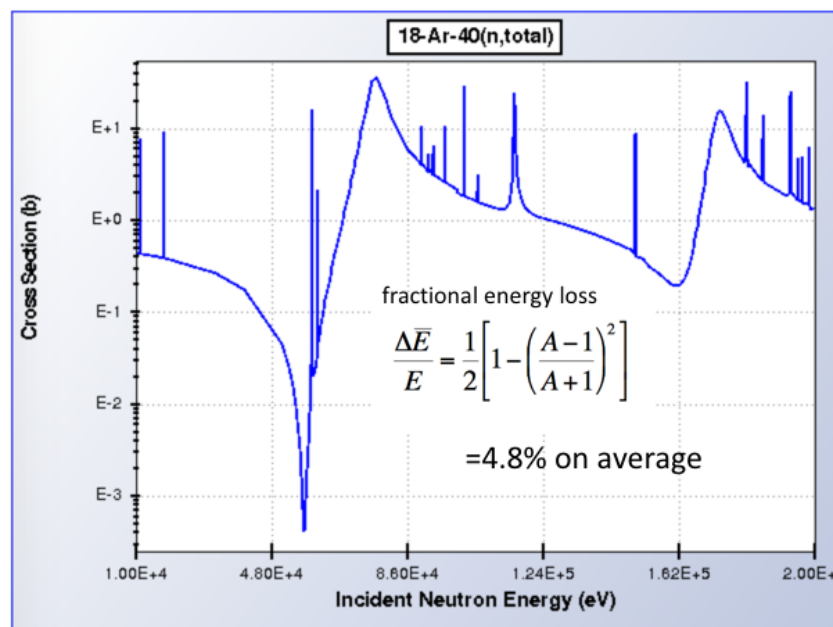


Figure 1.8: Total scattering cross sections on ^{40}Ar in the range $10 - 200\text{ keV}$ [?]

fig:Arxs

Therefore, estimating the width of the anti-resonance to be about 10 keV, a large fraction of the neutrons injected can be expected to fall into the cross section hole. Indeed, as will be shown in preliminary simulations, many neutrons scatter several times before escaping to lower energies to be captured. This simple phenomenon tends to scatter neutrons isotropically around the LAr.

The neutron capture gamma spectrum is also being characterized. In Nov 2017, the ACED Collaboration took several hundred thousand neutron capture events at the DANCE facility at LANSCE which will be used to prepare a database of the neutron capture gamma cascade chain.

1.6.4.2 Design Considerations

The fixed, shielded *DD* generator would be located above a feedthrough in the hydrogenous insulation. Pulsed⁴, commercially available *DD* generators exist and are cost competitive. Between the generator and the cryostat, layers of water or plastic and intermediate fillers will be included for sufficient degradation of the neutron energy. Initial simulations indicate that a single neutron injection point would illuminate the entire volume of one of the ProtoDUNE detectors. The *DD* generator itself is the size of a large thermos bottle. Space needed by the system will be determined by the desired shielding level which is yet to be understood.

1.6.4.3 Remaining Studies

The remaining studies for the TDR for the external neutron source are:

- Assessment of the full design, including degrader materials and shielding.
- Assessment of sufficient space and mounting (weight) considerations above the cryostat considering shielding for the neutron generator.

add more studies

⁴The pulse width is 100 μ s, but it is possible to reduce this by simply shortening the HV pulse that sustains the reaction.

Uploaded beginning of file to here 4/2/18 Anne; still to add in more sections

1.6.5 Photon Detection Monitoring System

1.6.5.1 Motivation and Possible Measurements

The primary function of the PDS in DUNE is to determine the $t0$ of an event to use as an input to the LArTPC reconstruction. A pulsed UV-light system, the same design deployed in the 35 ton prototype detector [45], is proposed as a way to cross-calibrate and monitor the PDs during commissioning and experimental operation. Such a calibration system would verify the dynamic range, the silicon photomultiplier (SiPM) gains and timing resolutions. The system would also evaluate the relative efficiencies of the detectors and monitor the stability and the response of the entire PDS as a function of time—for the duration of the experiment. The system would be capable of emitting light at various pulse heights and widths, and with a range of repetition rates (~ 1 Hz to a few kHz). The system is expected to help with studies of supernova-level signals and tests of trigger configuration by emitting light pulses at single- and multi-photoelectron levels with a well defined time difference between subsequent pulses. The system will not be used for absolute calibration; converting the number of photons to an ADC charge will use cosmic rays and the radioactive source system.

1.6.5.2 Design Considerations

This is for SP only; Need to clarify that through out the section. The PDS for DP system is covered under the DP-PDS consortium chapter. Will need to state that and link it from here.

The hardware consists of warm and cold components. By placing light sources with diffusers on the cathode planes, the system is designed to illuminate the PDs embedded in the APAs. Cold components of the calibration system (diffusers and fibers) interface with the HV system. These components will be installed with the CPA, and will go through FC strips and the GP. Diffusers are installed at each CPA, and therefore reside at the CPA potential. Insulating quartz fibers are used to transport light from optical feedthroughs (at the cryostat top) through the GP, and through FC strips to the CPA top frame. These fibers connect optically to diffusers located at CPA panels. Required fiber resistance is defined by HV system requirements to ensure that the cathode is protected from shorting due to fiber conductivity. An illustration of the proposed system is shown in Figure 1.9. This system with UV diffusers was tested successfully at the 35 ton prototype and was used in specialized runs such as the timing resolution measurement [45]. This system will also be deployed in the ProtoDUNE-SP.

Instead of, or in conjunction with the UV light system discussed in Section [?], the PDS may be used as a source of electrons on the cathode. A flash lamp would send light down the fiber, which would eject electrons from a small metal photo-cathode. This would provide a fixed source

- 3 within the detector with similar benefits as the UV light system, though with more limited spatial
4 granularity.

Figure 1.9: (Left) Illustration of the UV-light photon calibration system in the DUNE 35 ton prototype.
(Right) Diffuser mounted on the CPAs in the 35 ton prototype.

fig:pds

5 The calibration and the SP-PDS groups will define ports for optical feedthroughs. It is possible
6 that SP-PDS might use DSS ports or TPC signal ports for routing fibers. The calibration group
7 in coordination with other groups will provide a scheme for an interlock mechanism to be used
8 when operating various calibration devices (e.g., laser, radioactive sources) to avoid any damage
9 to the PDs. A dedicated firmware and software system will enable UV-light system to interface
10 with DAQ and slow controls to communicate the start and stop of calibration runs, and issue
11 commands to define types (amplitude, timing, frequency) of calibration pulses. Protocols will be
12 defined with the DAQ group.

13 1.6.5.3 Remaining Studies

14 The remaining studies for the photon calibration system prior to the TDR include:

- 15 • Testing of components of the proposed PD calibration system with ProtoDUNE. Additional
16 tests will be launched between the SP photon detector and HV groups as needed, including
17 a test stand with shared responsibility.
- 18 • Verification that the HV system operates without discharges that could cause light emission
19 observable by the PDS, should this be a concern.
- 1 • Operate the proposed photon calibration system in ProtoDUNE and define the related DAQ
2 needs for the Far Detector.

1.6.6 Cosmic Ray Tagger

1.6.6.1 Motivation and Possible Measurements

One of the standard tests for calibration involves using detector models to determine how well we reconstruct simulated events compared to detector events. This is the most direct way of estimating systematic errors on the model. This sort of test requires a way to constraint a track's position, direction, and time, independent of information from the detector itself. A *Cosmic Ray Tagger* (CRT), a dedicated fast tracking system, will provide such independent information from the TPC about neutrino-induced and cosmic-ray muon events. CRT-tagged tracks can also help test the E-field map in regions not illuminated well by the laser system. Additionally, a CRT can help diagnose problems such as displacement of cosmic-ray tracks due to drift field distortions and help with location tagging in the case of FC resistor failures since the CRT indicates exactly where the cosmics went.

Rock muons from beam interactions in the rock surrounding the cryostat have similar energy (up to losses in the rock) and angular (up to multiple scattering outside the cryostat) spectrum as CC ν_μ events. The number of rock muons entering the front face of the cryostat is similar to the number of CC ν_μ event rate contained in the detector. A nominal design of the CRT would cover the front face of the detector (approximately 14m \times 12m) to provide an estimate of the initial position, and the time for a subset of these events, independent of the TPC and PDS. A second, similarly sized panel, 1 m away from the cryostat would provide direction information. This is a critical test for reconstruction in the forward 1 m region of the detector, which can be compared with information from cosmic rays and other calibration sources. Additional measurements are possible elsewhere in the detector if the system is portable; it could be positioned on top of the cryostat to capture (nearly downward-going) cosmic rays during commissioning, or positioned along the side for rock muon-induced tracks along the drift direction.

Preliminary studies have shown that with about 100 rock muons (of the approximately 800 that will arrive in 1 year) it is possible to detect a 1% bias in rock-muon track reconstruction, which can be modeled as an error in the drift velocity v_d , at about the 2σ level. Confirmation of such a bias would directly impacts our estimates of the fiducial volume—the number of argon targets available for neutrino interactions in the detector. It also affects our estimates of backgrounds: the location of a π^0 decay must be known in order to determine the probability that one of its γ s converted in an inactive region of the detector (or exited).

1.6.6.2 Design Considerations

The CRT pixelization will be small enough that rock-muon statistics will allow determination of the center of each pixel to the same resolution as that expected for the detector (roughly 1 cm). So, for example, even with 50 one-cm-sized pixels, with about 1000 rock muons per year passing through the CRT, the achievable precision on average for the incident position (before subsequent multiple scattering) is about 5 mm. This assumes that the test integrates over all x and y , as doing the test in segments of x and y reduces the usable statistics. In addition to the pixelization that

- 3 will constrain x , y , z , and t for each track, placing a second, identical counter about 1 m upstream
4 will allow a measurement of the rock muon direction as well.
- 5 A concern is how such a system will be surveyed. Unlike APA and CPA crossers, these events
6 will depend only on the relative position of the CRT and the APA that observes the muon. Not
7 knowing these relative positions will compromise the precision of the measurement, and the error
8 in such a survey could be misinterpreted as a reconstruction bias.

9 1.6.6.3 Remaining Studies

10 The remaining studies for the CRT system prior to the TDR are:

- 11 • Continuation of simulation studies of the precision with which the CRT (including panels on
12 the sides and bottom) can determine biases or other problems with the detector model.,
- 13 • Continuation of size and pixelization optimization.
- 14 • Assessment of space surrounding the cryostat for the CRT, including space above (for cosmic
15 rays), along the side, or for a second panel 1 m away from the front face of the cryostat.
- 16 • Assessment of cost saving options, including reuse of existing scintillators (from MINOS), or
17 reuse of a counter system (e.g., from ProtoDUNE).
- 18 • As discussed above, a plan for surveying the CRT relative to the APAs also needs to be
19 developed, to be coordinated with the APA consortium.
- 1 • Continuation of discussions with the DAQ consortium on CRT needs, although this will
2 depend somewhat on the technology chosen.

1.7 Calibration Summary

The calibration needs for the DUNE detector modules are presented along with a strategy to meet them. An overview of existing sources and limitations in using those sources are also discussed. A set of proposed external calibration systems needed to meet DUNE's physics goals are presented. As listed, the calibration group will continue to pursue remaining studies with an aim to finalize the design considerations for calibration systems. Feedthrough accommodations are already made for the SP module to accommodate the proposed UV laser and radioactive source systems. The CRT and the neutron generator systems require more understanding in terms of the space constraints around the cryostat. More studies are also needed for the CRT system to finalize the size and placement of the system. In addition to the proposed systems, other systems are under consideration at an exploratory level. The need for these systems will be critically reviewed in the immediate future with a goal of finalizing the list of proposed systems in the near future. In the coming months, the calibration group will aim to finalize calibration penetrations for the DP module.

The calibration group has also started working closely with the consortia and identified liaisons for each. It is important to ensure that calibration needs are considered as each consortium develops its designs. A preliminary list of DAQ calibration requirements are already in process and will be finalized in the coming months. Additionally, more physics-driven studies are being launched to understand the impact of calibrations on long-baseline physics. As a first step, the calibration group has started collaborating with the long-baseline physics group to develop the necessary tools and techniques to propagate detector physics effects into oscillation analyses. Calibration tools developed in other experiments such as MicroBooNE will also be adopted for DUNE in the near future. The calibration group will also aim to increase dual phase participation to better understand calibration challenges for the DP design.

1.7.1 Path to the TDR

The calibration systems for DUNE, as presented in this document, will be further discussed and developed for the TDR within DUNE's management structure. Two options are currently favored for calibration, (1) formation of a new Calibration consortium, or (2) inclusion of calibration in the Cryogenic Instrumentation and Slow Controls (CISC) consortium. This decision will depend on the scope of the proposed calibration systems presented in this document. The goal is to make and execute this decision in June 2018, shortly after the final Technical Proposal submission. The full design development for each calibration system, along with costing and risk mitigation, will follow. For the TDR, the overall detector calibration strategy for the SP design (low-level calibration systems and physics-based) will be presented in a *Calibration Strategy* chapter of Volume 3 of the TDR. Details of the hardware will be presented in the corresponding consortium volume of the TDR. A similar structure is envisioned for the DP module. The Physics Volume of the TDR will contain a section discussing the physics-process based calibration measurements and the assumed systematic uncertainties that will be propagated to the physics sensitivities. Table 1.2 shows some high-level key milestones for calibration leading to the TDR.

Table 1.2: Key Calibration milestones leading to TDR.

Date	Milestone
Aug. 2017	Formation of Calibration Task Force
Dec. 2017	Finalize calibration penetrations for SP module
Jan. 2018	First proposal of calibration systems to the collaboration
Feb. 2018	Address calibration key questions and concerns
Mar. 2018	Calibration workshop – agree on proposed systems
May 2018	Technical Proposal
June 2018	Finalize process of integrating calibration into Consortium structure
Nov. 2018	Internal Review of Final Calibration System Design
Dec. 2018	Design validation using ProtoDUNE and SBN data (where applicable) and incorporate lessons learned into designs
Feb. 2019	Documentation of Final Design of all Calibration Systems
Apr. 2019	Technical Design Report
Oct. 2019	CD-2 DOE Review

References

- [1] DOE Office of High Energy Physics, “Mission Need Statement for a Long-Baseline Neutrino Experiment (LBNE),” tech. rep., DOE, 2009. LBNE-doc-6259.
- [2] **MicroBooNE** Collaboration, R. Acciarri *et al.*, “Michel Electron Reconstruction Using Cosmic-Ray Data from the MicroBooNE LArTPC,” *JINST* **12** no. 09, (2017) P09014, [arXiv:1704.02927 \[physics.ins-det\]](#).
- [3] **DUNE** Collaboration, R. Acciarri *et al.*, “Long-Baseline Neutrino Facility (LBNF) and Deep Underground Neutrino Experiment (DUNE),” [arXiv:1512.06148 \[physics.ins-det\]](#).
- [4] Worcester, E., “Energy Systematics Studies,” 2016.
<https://cdcv.s.fnal.gov/redmine/projects/lbne-beamsim/wiki>.
- [5] **LArIAT** Collaboration, F. Cavanna, M. Kordosky, J. Raaf, and B. Rebel, “LArIAT: Liquid Argon In A Testbeam.” [arXiv:1406.5560](#), 2014.
- [6] **MicroBooNE** Collaboration, R. Acciarri *et al.*, “Design and Construction of the MicroBooNE Detector,” *JINST* **12** no. 02, (2017) P02017, [arXiv:1612.05824 \[physics.ins-det\]](#).
- [7] **LAr1-ND, ICARUS-WA104, MicroBooNE** Collaboration, M. Antonello *et al.*, “A Proposal for a Three Detector Short-Baseline Neutrino Oscillation Program in the Fermilab Booster Neutrino Beam,” [arXiv:1503.01520 \[physics.ins-det\]](#).
- [8] A. Bolozdynya *et al.*, “Opportunities for Neutrino Physics at the Spallation Neutron Source: A White Paper,” 2012. [arXiv:1211.5199 \[hep-ex\]](#).
<http://inspirehep.net/record/1203677/files/arXiv:1211.5199.pdf>.
- [9] Yang, T. and Baller, B., “Event reconstruction improvements for $p \rightarrow \text{nubar } K^+$,” 2017.
<https://indico.fnal.gov/getFile.py/access?contribId=102&sessionId=14&resId=0&materialId=slides&confId=10641>.
- [10] **WArP** Collaboration, R. Acciarri *et al.*, “Effects of Nitrogen contamination in liquid Argon,” *JINST* **5** (2010) P06003, [arXiv:0804.1217 \[nucl-ex\]](#).

- [11] B. J. P. Jones, T. Alexander, H. O. Back, G. Collin, J. M. Conrad, A. Greene, T. Katori, S. Pordes, and M. Toups, “The Effects of Dissolved Methane upon Liquid Argon Scintillation Light,” *JINST* **8** (2013) P12015, [arXiv:1308.3658](#) [[physics.ins-det](#)].
- [12] G. Cancelo, F. Cavanna, C. O. Escobar, E. Kemp, A. A. Machado, A. Para, E. Segreto, D. Totani, and D. Warner, “Increasing the efficiency of photon collection in LArTPCs: the ARAPUCA light trap,” *JINST* **13** no. 03, (2018) C03040, [arXiv:1802.09726](#) [[physics.ins-det](#)].
- [13] Z. Moss, J. Moon, L. Bugel, J. M. Conrad, K. Sachdev, M. Toups, and T. Wongjirad, “A Factor of Four Increase in Attenuation Length of Dipped Lightguides for Liquid Argon TPCs Through Improved Coating,” [arXiv:1604.03103](#) [[physics.ins-det](#)].
- [14] Z. Moss, L. Bugel, G. Collin, J. M. Conrad, B. J. P. Jones, J. Moon, M. Toups, and T. Wongjirad, “Improved TPB-coated Light Guides for Liquid Argon TPC Light Detection Systems,” *JINST* **10** no. 08, (2015) P08017, [arXiv:1410.6256](#) [[physics.ins-det](#)].
- [15] **ArgoNeuT** Collaboration, R. Acciarri *et al.*, “A study of electron recombination using highly ionizing particles in the ArgoNeuT Liquid Argon TPC,” *JINST* **8** (2013) P08005, [arXiv:1306.1712](#) [[physics.ins-det](#)].
- [16] **ICARUS** Collaboration, S. Amoruso *et al.*, “Study of electron recombination in liquid argon with the ICARUS TPC,” *Nucl. Instrum. Meth.* **A523** (2004) 275–286.
- [17] M. Antonello, B. Baibussinov, P. Benetti, F. Boffelli, A. Bubak, *et al.*, “Experimental observation of an extremely high electron lifetime with the ICARUS-T600 LAr-TPC,” *JINST* **9** no. 12, (2014) P12006, [arXiv:1409.5592](#) [[physics.ins-det](#)].
- [18] T. M. Collaboration, “A Measurement of the Attenuation of Drifting Electrons in the MicroBooNE LArTPC,” tech. rep., 2017. MICROBOONE-NOTE-1026-PUB.
- [19] Y. Li *et al.*, “Measurement of Longitudinal Electron Diffusion in Liquid Argon,” *Nucl. Instrum. Meth.* **A816** (2016) 160–170, [arXiv:1508.07059](#) [[physics.ins-det](#)].
- [20] T. K. Warburton, *Simulations and Data analysis for the 35 ton Liquid Argon detector as a prototype for the DUNE experiment*. PhD thesis, Sheffield U., 2017. <http://lss.fnal.gov/archive/thesis/2000/fermilab-thesis-2017-28.pdf>.
- [21] T. M. Collaboration, “Study of Space Charge Effects in MicroBooNE,” tech. rep., 2016. <http://microboone.fnal.gov/wp-content/uploads/MICROBOONE-NOTE-1018-PUB.pdf>. MICROBOONE-NOTE-1018-PUB.
- [22] **ArgoNeuT** Collaboration, C. Anderson *et al.*, “Analysis of a Large Sample of Neutrino-Induced Muons with the ArgoNeuT Detector,” *JINST* **7** (2012) P10020, [arXiv:1205.6702](#) [[physics.ins-det](#)].
- [23] T. M. Collaboration, “Establishing a Pure Sample of Side-Piercing Through-Going

- 3 Cosmic-Ray Muons for LArTPC Calibration in MicroBooNE,” tech. rep., 2017.
4 <http://microboone.fnal.gov/wp-content/uploads/MICROBOONE-NOTE-1028-PUB.pdf>.
5 MICROBOONE-NOTE-1028-PUB.
- 6 [24] M. Auger *et al.*, “A Novel Cosmic Ray Tagger System for Liquid Argon TPC Neutrino
7 Detectors,” *Instruments* **1** no. 1, (2017) 2, [arXiv:1612.04614 \[physics.ins-det\]](#).
- 8 [25] A. Ereditato, D. Goeldi, S. Janos, I. Kreslo, M. Luethi, C. Rudolf von Rohr, M. Schenk,
9 T. Strauss, M. S. Weber, and M. Zeller, “Measurement of the drift field in the
10 ARGONTUBE LAr TPC with 266 nm pulsed laser beams,” *JINST* **9** no. 11, (2014) P11010,
11 [arXiv:1408.6635 \[physics.ins-det\]](#).
- 12 [26] **MicroBooNE** Collaboration, J. Conrad, B. J. P. Jones, Z. Moss, T. Strauss, and M. Touns,
13 “The Photomultiplier Tube Calibration System of the MicroBooNE Experiment,” *JINST* **10**
14 no. 06, (2015) T06001, [arXiv:1502.04159 \[physics.ins-det\]](#).
- 15 [27] **MicroBooNE** Collaboration, R. Acciarri *et al.*, “Convolutional Neural Networks Applied to
16 Neutrino Events in a Liquid Argon Time Projection Chamber,” *JINST* **12** no. 03, (2017)
17 P03011, [arXiv:1611.05531 \[physics.ins-det\]](#).
- 18 [28] **ICARUS** Collaboration, A. Ankowski *et al.*, “Measurement of through-going particle
19 momentum by means of multiple scattering with the ICARUS T600 TPC,” *Eur.Phys.J.*
20 **C48** (2006) 667–676, [arXiv:hep-ex/0606006 \[hep-ex\]](#).
- 21 [29] **ICARUS** Collaboration, M. Antonello *et al.*, “Muon momentum measurement in
22 ICARUS-T600 LAr-TPC via multiple scattering in few-GeV range,” *JINST* **12** no. 04,
23 (2017) P04010, [arXiv:1612.07715 \[physics.ins-det\]](#).
- 24 [30] **MicroBooNE** Collaboration, P. Abratenko *et al.*, “Determination of muon momentum in
25 the MicroBooNE LArTPC using an improved model of multiple Coulomb scattering,”
26 *JINST* **12** no. 10, (2017) P10010, [arXiv:1703.06187 \[physics.ins-det\]](#).
- 27 [31] **ICARUS Collaboration** Collaboration, S. Amoroso *et al.*, “Measurement of the mu decay
28 spectrum with the ICARUS liquid argon TPC,” *Eur.Phys.J.* **C33** (2004) 233–241,
29 [arXiv:hep-ex/0311040 \[hep-ex\]](#).
- 30 [32] **ICARUS** Collaboration, A. Ankowski *et al.*, “Energy reconstruction of electromagnetic
31 showers from π^0 decays with the ICARUS T600 Liquid Argon TPC,” *Acta Phys. Polon.*
32 **B41** (2010) 103–125, [arXiv:0812.2373 \[hep-ex\]](#).
- 33 [33] **ArgoNeuT** Collaboration, R. Acciarri *et al.*, “Measurement of ν_μ and $\bar{\nu}_\mu$ neutral current
34 $\pi^0 \rightarrow \gamma\gamma$ production in the ArgoNeuT detector,” *Phys. Rev.* **D96** no. 1, (2017) 012006,
35 [arXiv:1511.00941 \[hep-ex\]](#).
- 1 [34] **DUNE** Collaboration, B. Abi *et al.*, “The Single-Phase ProtoDUNE Technical Design
2 Report,” [arXiv:1706.07081 \[physics.ins-det\]](#).

- [35] D. Caratelli, *Study of Electromagnetic Interactions in the MicroBooNE Liquid Argon Time Projection Chamber*. PhD thesis, Columbia U., 2018.
<http://lss.fnal.gov/archive/thesis/2000/fermilab-thesis-2018-02.pdf>.
- [36] J. K. V. Kudryavtsev, M. Richardson and T. K. Warburton, “Muon simulations for lbne using music and musun,” tech. rep., 2014. LBNE-doc-9673.
- [37] V. A. Kudryavtsev, “Muon simulation codes MUSIC and MUSUN for underground physics,” *Comput. Phys. Commun.* **180** (2009) 339–346, [arXiv:0810.4635](https://arxiv.org/abs/0810.4635) [physics.comp-ph].
- [38] V. Lacuesta Miquel, *Alignment of the ATLAS Inner Detector and Single Top studies*. PhD thesis, Valencia U., IFIC, 2015.
http://inspirehep.net/record/1429422/files/fulltext__tA3vb.pdf.
- [39] R. Moles-Valls, *Inner detector alignment and top-quark mass measurement with the ATLAS detector*. PhD thesis, Valencia U., IFIC, 2014-02-19.
<http://inspirehep.net/record/1339828/files/CERN-THESIS-2014-145.pdf>.
- [40] CMS Collaboration, S. Chatrchyan *et al.*, “Alignment of the CMS Muon System with Cosmic-Ray and Beam-Halo Muons,” *JINST* **5** (2010) T03020, [arXiv:0911.4022](https://arxiv.org/abs/0911.4022) [physics.ins-det].
- [41] ALICE Collaboration, K. Aamodt *et al.*, “Alignment of the ALICE Inner Tracking System with cosmic-ray tracks,” *JINST* **5** (2010) P03003, [arXiv:1001.0502](https://arxiv.org/abs/1001.0502) [physics.ins-det].
- [42] Diurba, R., “Estimating the Rock Muon Rate from the Neutrino Beam at the DUNE FD,” tech. rep., 2018. DUNE DocDB 6628 v1.
- [43] M. Zeller *et al.*, “First measurements with ARGONTUBE, a 5m long drift Liquid Argon TPC,” *Nucl. Instrum. Meth.* **A718** (2013) 454–458.
- [44] T2K ND280 TPC Collaboration, N. Abgrall *et al.*, “Time Projection Chambers for the T2K Near Detectors,” *Nucl. Instrum. Meth.* **A637** (2011) 25–46, [arXiv:1012.0865](https://arxiv.org/abs/1012.0865) [physics.ins-det].
- [45] D. L. Adams *et al.*, “Photon detector system performance in the DUNE 35-ton prototype liquid argon time projection chamber,” [arXiv:1803.06379](https://arxiv.org/abs/1803.06379) [physics.ins-det].